LUND
UNIVERSITY

Lund Tekniska Högskola (LTH)

Microbial transformation of 5-hydroxymethylfurfural (HMF) to 2,5-Bis(hydroxymethyl)furan (BHMF).

by

Faqiha Ali Hamza

Department of Biotechnology - Master Thesis 2024

Supervisor: Sang Hyun Pyo
Co-Supervisor: Mahmoud Syed Ali Sayed
Examiner: Javier Linares Pasten

Abstract

The chemical industry is particularly resource-intensive, consuming a substantial portion of petroleum resources and significantly contributing to greenhouse gas emissions. Consequently, there is an urgent need to explore sustainable alternatives. Biomass has emerged as a promising renewable resource. The dehydration of biomass-derived carbohydrates has proven to be an effective method, producing key intermediates such as 5-hydroxymethylfurfural (HMF). HMF is a versatile platform chemical that paves the way for various valuable bioproducts, providing a sustainable solution to reduce reliance on fossil fuels and mitigate environmental impacts.

This study focuses on using *Mycobacterium* MS1601, a bacterium identified for its natural ability to reduce HMF to BHMF through whole-cell catalysis. This study focused on optimizing the bioconversion of 5-hydroxymethylfurfural (HMF) to 2,5-bis(hydroxymethyl)furan (BHMF) using Mycobacterium sp. MS1601. Key parameters such as incubation duration, carbon source, pH, cell concentration, substrate concentration, and anaerobic conditions were evaluated. Glucose emerged as the optimal carbon source, achieving a 63.2% BHMF yield at pH 7 within 24 hours. A cell concentration of 50 gCDW/L significantly improved BHMF yield to 80.8%, while NADH supplementation did not enhance production. Lower substrate concentrations were found to be optimal, and aerobic conditions favored higher yields. Upscale bioreactor experiments demonstrated significant improvements in BHMF production, achieving a rapid increase from 9.8% to 63.0% over 24 hours. BHMF was successfully purified using liquid-liquid extraction followed by flash chromatography. Additionally, a potential dehydrogenase gene responsible for HMF reduction was identified, amplified, and cloned, providing a basis for future genetic optimization and industrial applications

These findings highlight the potential of *Mycobacterium* sp. MS1601 as a robust biocatalyst for sustainable BHMF production. The study's optimized conditions and gene identification provide a foundation for future genetic enhancements and industrial applications. This research contributes to the development of environmentally friendly processes, offering a viable alternative to fossil-based chemicals and paving the way for greener industrial practices.

Table of Contents

Abstract 2

Abbreviations 5

1. Introduction 6

1.1. 5-hydroxymethylfurfural (HMF) 6

1.2. 2,5-bis(hydroxymethyl)furan (BHMF) 7

1.2.1. Applications 7

1.2.2. BHMF Synthesis 9

2. Materials and Methods 12

Mycobacterium MS1601 reduction reactions 13

2.1.1. Incubation time and carbon source screening 13

2.1.2. pH screening 13

2.1.3. NADH supplementation 13

2.1.4. Cell concentration screening 13

2.1.5. Substrate concentration screening 14

2.1.6. Anaerobic Reaction 14

2.1.7. Upscale Reaction 14

2.1.8. OD vs Time 14

Extraction and purification of BHMF 14

Gene Identification 15

2.1.9. Gene Amplification 15

2.1.10. Digestion and Ligation 15

2.1.11. Transformation 15

3. Results and Discussion 16

Mycobacterium MS1601 reduction reactions 16

3.1.1. Incubation time and carbon source screening 16

3.1.2. pH screening 18

3.1.2. NADH supplementation 19

3.1.3. Cell concentration screening 20

3.1.4. Substrate concentration screening 21

3.1.5. Anaerobic Reaction 23

3.1.6. Upscale Bioreactor Reaction 24

3.1.7. OD vs Time 25

Extraction and Purification of BHMF 26

3.1.8. Flash Column Chromatography 26

3.1.2. NMR 27
Molecular Analysis 28
3.1.3. Amplification and Gel Electrophoresis 28
3.1.4. Cloning and Transformation 29
Conclusion 30
References 31
Appendix 35

Abbreviations

HMF	*5-hydroxymethylfurfural*
BHMF	*2,5-bis(hydroxymethyl)furan*
HMFCA	*5-Hydroxymethyl-2-furan carboxylic acid*
FDCA	*2,5-furandicarboxylic acid*
FFCA	*5-Formyl-2-furancarboxylic Acid*
NADH	*Nicotinamide adenine dinucleotide (reduced form)*
PCR	*Polymerase chain reaction*
TLC	*Thin layer chromatography*

1. Introduction

The growing demand for energy and materials, driven by population expansion and consumer habits, has placed immense pressure on non-renewable fossil resources, resulting in significant depletion and escalating environmental concerns **(Scheme 1).** Chemical production requires at least 10% of the petroleum resources which is estimated to increase to 20% by 2040 contributing to about 16% greenhouse gas emissions (GHG) (Davidson et al., 2021). This has become a driving force in finding alternative sources for chemicals and fuels that are not only green and sustainable but also abundant to counter the impacts of the chemical production environment in the long term (H. Xia et al., 2018). Biomass shines like a star in the world of biotechnology when it comes to renewable fuel and chemical resources. It is not the only renewable organic carbon source but also the biggest next to coal and oil and has an estimated production of 1.0×10^{11} tons per year (Z. Zhang & Zhao, 2010).

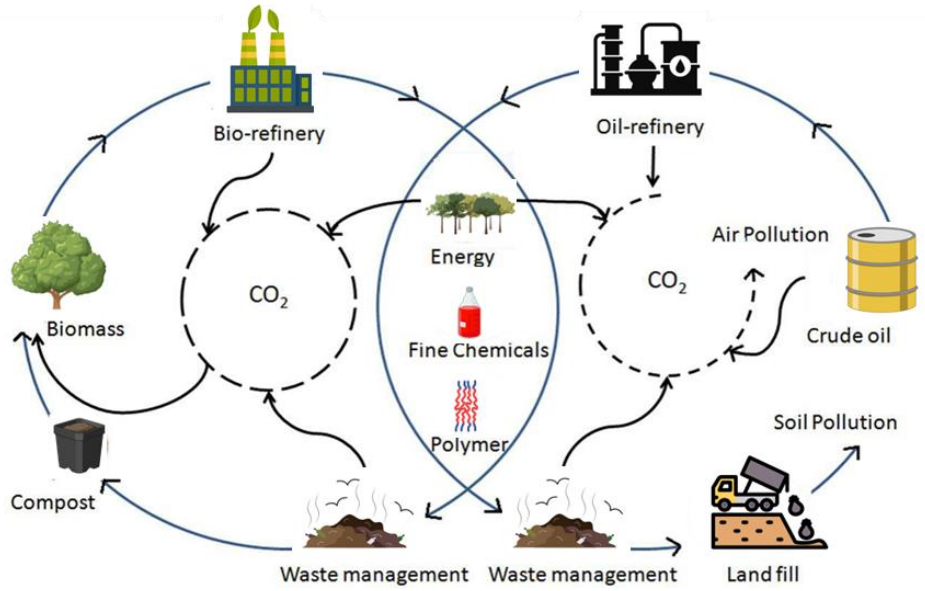

Scheme 1: *Impact of a bio-based refinery versus a fossil resources-based refinery (Vaidyanathan et al., 2023).*

1.1. 5-hydroxymethylfurfural (HMF)

An organic furan compound called 5-hydroxymethylfurfural (HMF) ($C_6H_6O_3$), produced from a hexose (fructose, glucose and higher saccharides), efficiently retaining all six Carbons is one such compound that has been recognised by the US Department of Energy as one of the best biobased platform chemicals that poses no harm to humans or environment.

HMF can be commonly found in in various items in our daily diet such as coffee, bread, biscuits, cereal and beer among many other products. Whenever these foods are heated, HMF is produced. About 5-150 mg is consumed daily per person (Shapla et al., 2018). HMF has been extensively under study since the last two decades, where both production of HMF and as well as its derivatives have been of great interest (Pyo et al., 2019) (Sayed et al., 2020). HMF can undergo various reactions, such as hydrogenation, oxidation, esterification, and hydrolysis and produce a variety of value-added chemicals, such as furan-2,5-dicarbaldehyde (FFCA), 2,5-furandicarboxylic acid (FDCA) and its esters, bis(hydroxymethyl)furan (BHMF) (Menegazzo et al., 2018) **(Scheme 2)**. Both biological conversion and catalytic conversion methods have been employed to produce different derivatives. HMF is an interesting

compound that holds hydroxyl, furan, and aldehyde units which lends itself to further modification into useful products. However, HMF is not an easy compound to work with due to its low stability (sensitive to oxygen, acids and bases) and high cost (Menegazzo et al., 2018). In pursuit of optimizing the compound, the discovery of many derivatives came into being such as 2,5 furandicarboxylic acid (FDCA) (Prasad et al., 2023), 5-formyl-2-furancarboxylic acid (FFCA) (J. Xu et al., 2019), 2,5-bis(hydroxymethyl)furan (BHMF) emerging as prominent examples (Scheme 2). These derivatives offer diverse applications within the biobased industries, promising solutions to address the limitations posed by HMF's inherent properties.

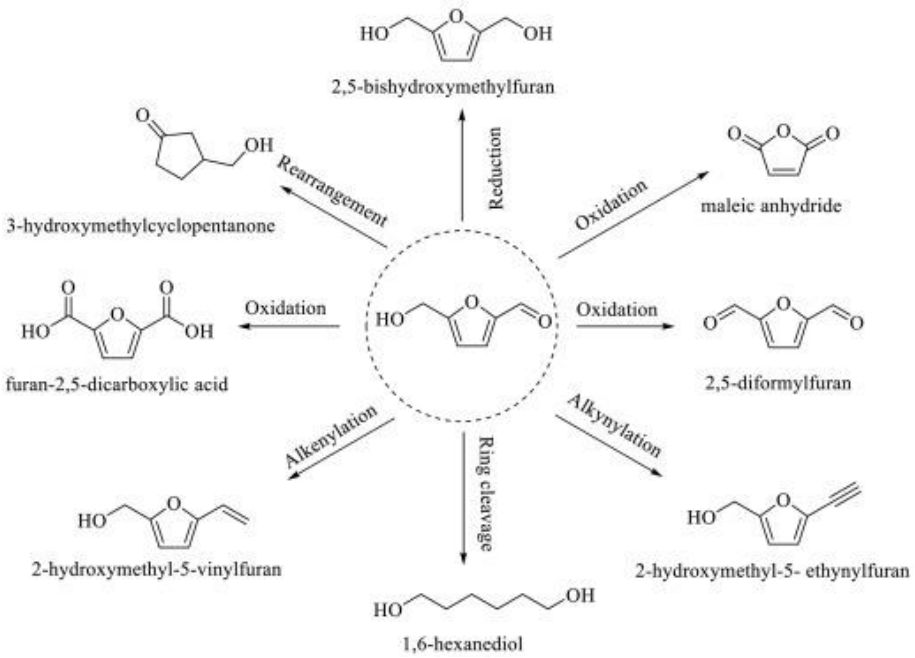

Scheme 2: *HMF and its furan derivatives (Kong et al., 2020)*

1.2. 2,5-bis(hydroxymethyl)furan (BHMF)

BHMF, a heterocyclic furan compound obtained via reduction of the formyl group of HMF, and structurally very similar to FDCA, has gained a lot of attention in recent years. BHMF can serve as a foundational component for plasticizers, biodiesel enhancers, flame retardants, and surfactants. BHMF like FDCA, is much more chemically and thermally stable than HMF (Post et al., 2023).

1.2.1. Applications

Recent studies have demonstrated the versatility of BHMF in applications ranging from polymer synthesis to the creation of novel composites. For instance, BHMF has been effectively incorporated into urea-formaldehyde (UF) resins, enhancing their properties while reducing environmental impact. The compound's utility is further evidenced in the development of epoxy resins and polyurethanes that rival traditional phenol-based resins in terms of performance and safety (F. Hu et al., 2016).

Furthermore, BHMF's role extends beyond typical polymer applications; it has been used to develop eco-friendly polyurethane products with self-healing and recyclable properties (Zhang et al., 2019). Researchers have also explored its potential in forming non-isocyanate polyurethanes (NIPUs), highlighting its adaptability and sustainability. The synthesis of BHMF-based esters and their application as non-ionic surfactants and biodiesel additives

underline the compound's broad utility, reflecting its integration into various industrial applications.

100 % BHMF-based polyester is a difunctional compound, meaning it possesses two reactive functional groups, that need another difunctional comonomer build polyesters, such as other diacid or a dimethyl ester (for example succinic acid and adipic acid). **Table 1** shows several comonomers, and catalysts reaction conditions reported in literature to produce BHMF-based furanic polyesters (Post et al., 2023).

Table 1: *Several BHMF based furanic Polyesters (Post et al., 2023).*

Comonomers	Catalysts	Conditions	M_n (g/mol)	T_g (°C)	T_m (°C)	Source
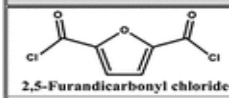 2,5-Furandicarbonyl chloride	Tetrabutyl-ammonium bromide	NaOH (water)/ DCM RT, 1h	3880	n.d.[d]	n.d.	Gomes (2011)[46]
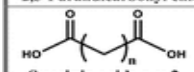 Succinic acid: n = 2	DMAP, DIC[b]	RT, 24h, N_2	5100 - 5700	13	89	Zeng, Ikezaki (2013, 2014)[44,54]
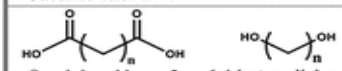 Succinic acid: n = 2 1,4-butanediol: n = 4	DMAP, DIC	RT, 24h, N_2	4300 - 7200	-30 - 2	91	Ikezaki (2014)[54]
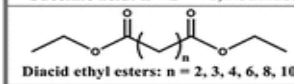 Diacid ethyl esters: n = 2, 3, 4, 6, 8, 10	iCALB[c]	80°C, 1) N_2 2h 2) 350 mmHg 4h 3) 2 mmHg 66h	2100 - 2400	-38 - 4	43 - 86	Jiang (2014)[50]
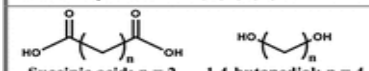 Succinic acid: n = 2 1,4-butanediol: n = 4	DMAP, DIC	PFS / PBS: RT, 24 h / 220 °C 2h Polymerization: 130 °C 1h	43 600 - 55 300	-25 - -3	105 - 106	Zhang (2017)[43]
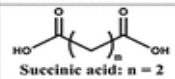 Succinic acid: n = 2	DMAP, DIC	RT, 24h, N_2 (1-butanol)	2700	n.d.	99	Upare (2018)[47]
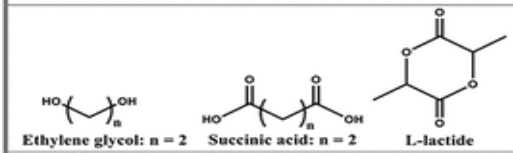 Ethylene glycol: n = 2 Succinic acid: n = 2 L-lactide	DMAP, DIC	RT, 24h, N_2	5000 - 14 600	16 - 34	n.d.	Cai (2019)[58]
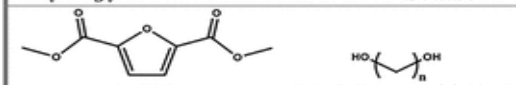 DMFDCA Aliphatic diol: n = 4, 6, 8, 10, 12	iCALB	80°C, 1) N_2 2h 2) 2 mmHg 48h 95 °C, 3) vacuum 24h	1400 - 16 050	-2 - 15	88 - 142	Maniar (2019)[51]
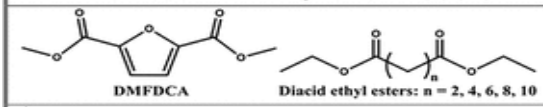 DMFDCA Diacid ethyl esters: n = 2, 4, 6, 8, 10	iCALB	80°C, 1) N_2 2h 2) 2 mmHg 48h 95°C, 3) vacuum 24h	600 - 8900	-19 - -6	57 - 79	Maniar (2019)[51]
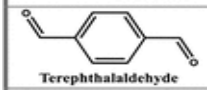 Terephthalaldehyde	DBU, Triazolium salt	RT, 16h, Ar	3100	60	181	Ragno (2019)[48]
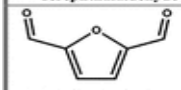 2,5-diformylfuran	DBU, Triazolium salt	RT, 16h, Ar	7800	n.d.	n.d.	Ragno (2019)[48]
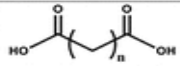 Diacid: n = 2, 4, 8	iCALB	85°C, 1) 1 bar 6h 2) 20 mbar 90h	2800 - 3100	-22 - 10	81	Pellis (2020)[52]
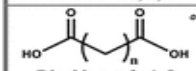 Diacid: n = 2, 4, 8	iCALB	85°C, 1) 1 bar 6h 2) 20 mbar 90h	600 - 1000	-1 - -39	170 - 189	Pellis (2020)[52]
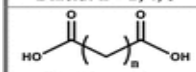 Diacid: n = 4, 5	$MgCl_2$, (TMP)MgCl·LiCl	30 - 80°C, N_2 15 - 115h	1800 - 6400	-23 - -9	42-47	Guillaume (2021)[49]

There are two patents for synthesizing monoesters to produce non-ionic surfactants. One patent involves the chemo-catalytic diesterification of BHMF with free fatty acids, while the other patent describes the chemo-catalytic esterification using free fatty acids with HMF, BHMF, and hydrogenated furans combined (Stensrud et al., 2014).

Another study was done to produce efficient BHMF-based fatty acid diesters as low-grade biodiesel additives, involving enzymatic double esterification of BHMF and saturated long fatty acid chains (Lăcătuş et al., 2018). BHMF can also serve as a base for plasticizers, such as those used in poly (vinyl chloride) (PVC). To render PVC highly flexible, a multitude of plasticizers, including phthalic acid esters, are employed. Among the most prevalent plasticizers/phthalates utilized in PVC production is Di(2-ethylhexyl) phthalate (DEHP). However, these phthalates pose significant risks to human health and are linked to various diseases stemming from endocrine disruption. Exposure to these phthalates has become pervasive, as they are commonly found in numerous everyday items including toys, medical devices, packaging, and more. Regulatory measures have been enacted to restrict the use of phthalates, prompting endeavors to discover safer, biobased alternatives that are free from adverse effects on human health and the environment. **Table 2** shows several biobased esters synthesized with BHMF that have demonstrated comparable quality to PVC matrices (Howell & Lazar, 2018).

Table 2: *BHMF based Esters with plasticizing effectiveness in PVC.*

Ester	Designation	Physical Form, Melting Point (°C)
bis-2,5-(2-Ethylhexanoylmethyl)furan (1)	BHMF-E	Liquid
bis-2,5-(Octanoylmethyl)furan (3)	BHMF-O	Solid, 29
bis-2,5-(2-Phenylacetoxymethyl)furan (6)	BHMF-P	Solid, 66
bis-2,5-(Benzoylmethyl)furan (4)	BHMF-B	Solid, 77
bis-2,5-(Stearoylmethyl)furan (2)	BHMF-S	Solid, 78
bis-2,5-(Dodecanoylmethyl)furan (5)	BHMF-D	Solid, 58

1.2.2. BHMF Synthesis

There are many ways in which BHMF has been produced, following are some of them (**Scheme 3):**

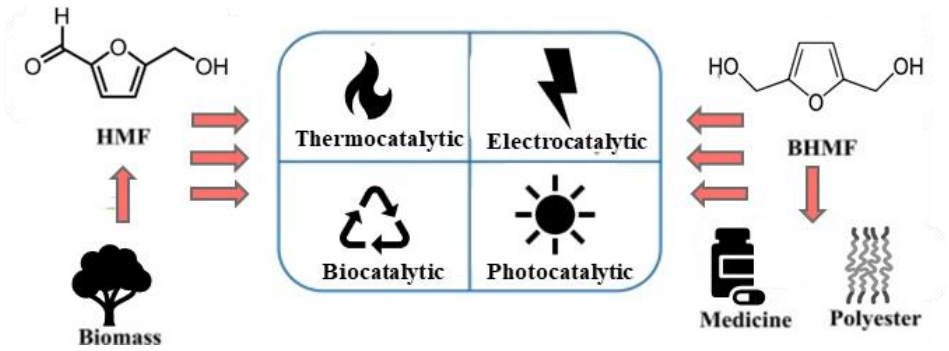

Scheme 3: *Four Catalytic Methods for Converting HMF to BHMF (Zhao et al., 2023).*

Thermocatalytic Hydrogenation

Thermocatalytic hydrogenation of HMF into BHMF is categorized into precious and non-precious metals based on catalytic activity. Precious metal catalysts, such as Ru, Rh, Ir, Au, Pd, and Pt, are known for their high hydrogenation activity, with Ru-based catalysts being the most extensively studied (Alamillo et al., 2012) (Mishra et al., 2020) (Han et al., 2016b). Ru catalysts supported on various materials have achieved up to 99% BHMF yields under specific conditions (Han et al., 2016). Similarly, Pt (98.9% BHMF yield) and Au (96 % BHMF yield) catalysts exhibit remarkable selectivity and efficiency, although the high cost and poor recyclability of some precious metal catalysts pose challenges (Chatterjee et al., 2014) (Liu et al., 2014) (Ohyama et al., 2016). In contrast, non-precious metal catalysts, including Cu, Zr, Co, Hf, and Ni, are being developed for their cost-effectiveness and competitive catalytic properties (Zhu et al., 2015) (H. Li et al., 2016) (Wang et al., 2016) (Hu et al., 2019) (Z. Liu et al., 2022). Cu-based catalysts show high reactivity towards C=O bonds, achieving significant BHMF yields under optimized conditions. The use of alcohols as hydrogen donors in Zr-based catalysts and the development of bimetallic catalysts enhance catalytic performance and stability. Additionally, the size of metal particles significantly influences catalytic properties, with smaller particles generally exhibiting higher activity (Zhao et al., 2023).

Electrocatalytic Hydrogenation:

Electrocatalytic hydrogenation utilizes applied potentials to drive the reduction of HMF to BHMF. Ag-based catalysts demonstrate high selectivity and efficiency. For example, Ag/Cu catalysts achieved a 86% of BHMF generation at −1.3 V (De Luna et al., 2021). Electrocatalytic pathways offer the advantage of mild reaction conditions, avoiding high temperatures and pressures. By controlling the electrochemical potential and Faradaic current, the reaction rate and selectivity can be finely tuned.

Photocatalytic Hydrogenation:

Photocatalytic methods use light energy to reduce HMF (C. Li & Na, 2021). Photocatalysts like Pt/g-C3N4 and Au/SiC show potential, although challenges remain in improving product selectivity and industrial scalability (Guo & Chen, 2016) (Hao et al., 2016b). For instance, Au/SiC achieved an 83.7% yield of BHMF under Xe-lamp irradiation. Photocatalysis leverages solar energy, providing a sustainable and environmentally friendly approach to hydrogenation. The development of efficient photocatalysts is crucial for the industrial application of this method.

Biocatalytic Hydrogenation

Biocatalysis involves using whole cells or isolated enzymes to convert HMF into BHMF. This method is particularly promising for its selectivity and ability to operate under environmentally benign conditions. Whole-cell biocatalysts offer advantages over enzyme biocatalysis, such as the regeneration of cofactors and ease of catalyst recycling. Microbial strains used in these processes are often genetically engineered to enhance their tolerance to HMF and to optimize their catalytic efficiency. Several microorganisms, including bacteria, yeast, and fungi, have been used to produce BHMF from HMF **(Table 3)**.

Bacteria: *Paraburkholderia azotifigens F18* produced 36.9 mM BHMF with a 92% yield in anaerobic batch processing (Xu et al., 2020). *Escherichia coli CCZU-K14,* modified with a reductase from *Candida magnoliae*, reached a 91% yield (He et al., 2018). *Burkholderia contaminans NJPI-15* achieved the highest titer of 656 mM BHMF with a 94% yield in fed-batch processing (Chang et al., 2021).

Yeast: *Meyerozyma guilliermondii SC110***3** achieved yields of 86% and ~88% in batch and fed-batch processes, respectively (Li et al., 2016b; Z. Xu et al., 2018). *Saccharomyces cerevisiae*, expressing an aryl alcohol dehydrogenase, produced BHMF with yields of 94% and ~77% in batch and fed-batch processes (Xia et al., 2020*). Kluyveromyces marxianus* demonstrated a 100% yield, producing 55.3 mM BHMF (Baptista et al., 2021).

Fungi*: Aureobasidium subglaciale F134* showed high productivity of 28.7 mM/h, yielding 430 mM BHMF (Chen et al., 2021). *Fusarium striatum* achieved a 97% yield, producing 145 mM BHMF (Millán et al., 2021).

Table 3: *Whole-cell biocatalysts reported for the conversion of 5-hydroxymethylfurfural (HMF) into2,5-bis(hydroxymethyl)furan (BHMF). Yield is presented as percentage of the theoretical molar yield. OD: optical density. CDW: cell dry weight (Cunha et al., 2022).*

Strain	Condition	Cell Inoculum	Medium	Initial HMF (mM)	Process	Final BHMF (mM)	Yield (%)	Productivity (mM/h)	Ref.
***Paraburkholderia azotifigens* F18**	30 °C, pH 7, 150 rpm	67 g/L wet cells	100 mM phosphate buffer with 40 mM glucose	40 mM	Batch, anaerobic	36.9	92	-	(Xu et al., 2020).
***Meyerozyma guilliermondii* SC1103**	35 °C, pH 7.2, 200 rpm	20 g/L wet cells	100 mM phosphate buffer with glucose	100	Batch	86	86	7.17	(Li et al., 2016b)
				50	Fed-batch: ~217 mM total HMF	191	~88	7.80	
***Meyerozyma guilliermondii* SC1103**	35 °C, pH 8, 200 rpm	20 g/L wet cells	100 mM Tris-HCl buffer with glucose	213	Batch. Cell acclimatization and immobilization calcium alginate beads	181	85	25.8	(Z. Xu et al., 2018)
Escherichia coli* CCZU-K14 harboring NADH-dependent reductase from *Candida magnoliae	30 °C, pH 6.5, 160 rpm	100 g/L wet cells	Glucose, xylose, l-glutamic acid, Mg2+, β-cyclodextrin, and CTAB	200	Batch.	181	91	2.51	(He et al., 2018)
Saccharomyces cerevisiae* harboring an aryl alcohol dehydrogenase from *M. guilliermondii	30 °C, pH 8, 200 rpm	60 g/L wet cells	100 mM Tris-HCl buffer and glucose	250	Batch	235	94	9.79	(Xia et al., 2020)
				150	Fed-batch: ~450 mM total HMF	345	~77	15.0	
***Aureobasidium subglaciale* F134**	30 °C, pH 7, 850 rpm	200 g/L wet cells	100 mM phosphate buffer with Zn2+ ion	180	Batch	148	82	16.4	(Chen et al., 2021)
				100	Fed-batch: ~500 mM total HMF	430	86	28.7	

Fusarium striatum	28 °C, pH 7, 160 rpm	4.0 × 106 spores/mL	Malt extract media with glucose	75	Fed-batch: 150 mM total HMF	145	97	2.42	(Millán et al., 2021)
***Burkholderia contaminans* NJPI-15**	35 °C, pH 7, 180 rpm	20 g/L wet cells	50 mM PBS with glutamine, sucrose and Mn2+	100	Batch	95	95	nd	(Chang et al., 2021)
				125	Fed-batch: 700 mM total HMF	656	94	13.7	
Kluyveromyces marxianus	37 °C, 150 rpm	100 g/L wet cells	YPD medium (111 mM glucose)	55.5	Batch	55.3	100	4.61	(Baptista et al., 2021)

Discovering a wild-type microorganism that is tolerant to HMF, which is typically toxic to most microbial cells, is highly advantageous for bioconversion processes. This study focuses on the reduction of HMF to BHMF via whole-cell catalysis by a *Mycobacterium* MS1601 bacterium identified by (Sayed et al., 2022). This bacterium is found to be rich in enzymes such as oxidases and dehydrogenases that can catalyze HMF into various derivatives (Sayed et al., 2017). By optimizing conditions, the reaction can be directed towards either reduction or oxidation. The primary aims of this study were: first, to enhance the cells' reduction power and make them more selective towards BHMF production; second, to achieve complete conversion of HMF in a relatively short time; and third, to extract and purify BHMF. Additionally, we aimed to identify the gene involved in BHMF production from HMF. An NADH-dependent carbonyl reductase (crs1) gene from *Candida*, was used as a reference sequence to identify the gene sequence in *Mycobacterium* responsible for the reduction of HMF (He et al., 2014).

2. Materials and Methods

To make preculture, 200µL of 20% glycerol sock of *Mycobacterium* sp. MS1601 were suspended in 10 ml Nutrient broth (composition per Litre: 5g peptone and 3 g beef extract (pH6.8)) in 250 ml baffled shake flasks. All flasks were incubated at 30 degrees for 24 hours in an orbital incubator at 200 rpm. This preculture was then transferred to an Activation media that container liter: 2g sodium acetate, 10 yeast extract, and 10 g carbon source. The activation media culture was then incubated at 30 degrees at 200 rpm. After incubation, the cells were centrifuged and washed with buffer to prepare for the transformation reaction. The cells were then subjected to a transformation reaction supplemented with HMF lasting 24 hours.

Reaction Analysis

The analysis for all reaction samples was performed using HPLC (LC-4000, Jasco, Japan), equipped with a Bio-Rad HPLC fast acid analysis column (100 × 7.8 mm), UV detector at 254 nm, and an autosampler. The column temperature was set to 65°C. Samples were diluted with Milli-Q water, mixed with 10% H_2SO_4, filtered, and a 10 µl aliquot was injected into the mobile phase (5 mM H_2SO_4) at a flow rate of 0.6 ml/min. Peaks were confirmed and quantified using external standards.

Mycobacterium MS1601 reduction reactions

2.1.1. Incubation time and carbon source screening

The experiment examined the influence of incubation durations of Activation median lasting 24 and 48, paired with three distinct carbon sources: glucose, glycerol, and sorbitol. *Mycobacterium* cells (preculture) were activated by growing over 24 hours and 48 hours in an Activation media. Three separate flasks were set up, each containing Activation media with different carbon source, that is Glucose, sorbitol and glycerol, 10g/L each, incubated at 30℃ in an incubator (INFORS HT, Ecotron). After the cells were activated for 24 hours and 48 hours, they were centrifuged and washed. Finally, three 2ml reactions (all duplicated) were set up at 30℃ at 500 rpm in a thermoshaker (MKR 13, HLC Biotech, Germany), each vial containing 20 g_{CDW}/L cells suspended in phosphate buffer (pH 7) along with 5g/L HMF as a substrate. Samples of 50 µl were taken at 0, 1 2, 3, 4, 6, 8, 9 and 24 hours for product and substrate analysis.

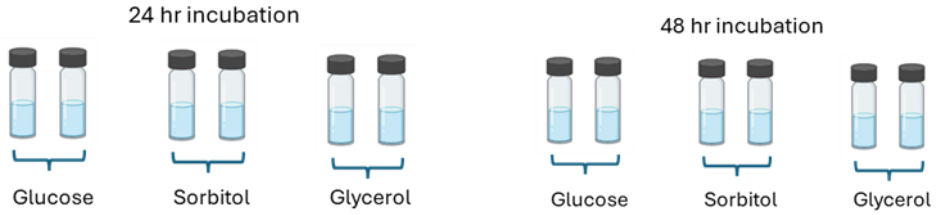

2.1.2. pH screening

The effect of pH values, 6, 7, and 8 of the reaction buffer was evaluated through activating the *Mycobacterium* cell in activation medium supplemented with 10 g/L glucose as carbon source for 24h. The reaction was initiated by suspending 20 g_{CDW}/L of cells in 10 ml phosphate buffer of pH 6, 7, and 8 and supplemented with 5g/L HMF in 50 ml falcon tube. All tubes were incubated at 30 ºC for 24h. Samples were collected within regular time and prepared for HPLC analysis.

2.1.3. NADH supplementation

The hydride ions donated by NADH actively engage in reducing the carbonyl group in HMF, leading to the formation of BHMF ($HMF + 2NADH + 2H^+ \rightarrow BHMF + 2NAD^+$). To improve the selectivity of our cells, we added NADH as a cofactor in the reaction along with HMF as the substrate. Both HMF and NADH were used in equimolar concentrations. Since 5 g/L of HMF is equivalent to 39.6 mM, an equal molar concentration of beta-Nicotinamide adenine dinucleotide, disodium salt, hydrate, 95+%, reduced form, was added to the reaction, corresponding to 28.098 g/L.

Prior to commencing the reaction, cells were activated in an activation media with glucose as the carbon source for 24 hours at 30 ºC. After centrifugation and washing, cells were lysed using a sonicator for 10 minutes. The 10 ml reaction mixture, consisting of 20 g_{CDW}/L of activated cells, 5 g/L HMF and 28.1 g/L NADH in a pH 7 phosphate buffer, was incubated at 30 ºC for 24 hours.

2.1.4. Cell concentration screening

Up until now, we have conducted reactions using a cell concentration of 20 gCDW/L. Now, cell concentrations of 50 g_{CDW} /L and 100 g_{CDW} /L were employed to evaluate their effects on the reaction. Cells were incubated in activation media containing glucose for 31 hours at

30ºC.Only changing the concentration of cells, all other reaction conditions remained constant: pH 7, 5 g/L HMF, and an incubation period of 24 hours at 30ºC.

2.1.5. Substrate concentration screening

The effect of different substrate concentrations on the reaction rate was screened through dissolving of 10g/L, 15g/L, 20g/L, and 25g/L HMF in 10 ml of phosphate buffer pH 7 in 50 ml falcon tubes. Each tube was supplemented with 5 mg/ml CDW of activated cell and the reaction was carried out under the same conditions mentioned in section 2.1.4. Samples of were collected in regular time for further analysis.

2.1.6. Anaerobic Reaction

To explore the potential of *Mycobacterium* MS1601cells for increasing the selectivity towards BHMF in the bioconversion of HMF, an experiment was conducted under strictly anaerobic conditions. The experiment utilized a cell concentration of 50 g/L, pH 7, with an incubation time of 31 hours in activated media, and an HMF concentration of 10 g/L in a 10 ml reaction volume.

2.1.7. Upscale Reaction

The last transformation experiment was an upscale experiment using the optimal conditions identified throughout previous experiment. 50 gcwd/L cells were suspended in 300 ml sodium phosphate buffer (pH 7) supplemented with 20 g/L HMF in a 1L bioreactor. Biotransformation reaction was performed at 30 °C, 250 rpm with pH continuously maintained at 7 using 1 M NaOH solution. Dissolved oxygen was maintained at 20% during the entire experiment by regulating the stirrer speed. The oxygen level was controlled at fixed aeration rate of 0.5. Two millilitre samples were collected during the reaction for analysing substrate and product concentrations at regular intervals.

2.1.8. OD vs Time

The growth of activation media inoculated with *Mycobacterium* MS1601 cells was monitored and recorded over 32 hours using a spectrophotometer at 600 nm to measure the optical density (OD).

Extraction and purification of BHMF

Once the reaction was concluded at 32 hours, the sample was centrifuged at 4500 rpm for 50 minutes to pellet down all the cells (Sorvall LYNX 4000, Thermo Scientific, Germany). The supernatant was frozen overnight followed by freeze drying using a Lyophilizer (Lyph Lock 12, Labconc) that continued for about two days. Once the sample was dried, the mixture was subjected to liquid-liquid extraction technique using ethyl acetate (Glaser et al., 2023). One millilitre ethyl acetate was added to the dried mixture and mixed thoroughly. The process was repeated twice. The liquid was then taken into a separate 2ml Eppendorf Tube. A Thin layer chromatography (TLC) was done to confirm if BHMF was extracted successfully. After every TLC, chemical classes were detected with ultraviolet light (254 nm) and a chemical developer stain called p-Anisaldehyde (Composition: 0.5ml p-Anisaldehyde mixed with 10ml acetic acid, 85ml methanol and 5ml concentrated sulphuric acid) (Kinghorn, 1997). To purify further, a flash column chromatography was performed with silica gel as solid phase and ethyl acetate and hexane as liquid phase. First Silica gel was dissolved in Hexane and was poured into the column (1 cm Diameter) up to 15 cm height. Once the silica was set, 2 ml sample mixture (obtained from liquid-liquid extraction) was poured carefully over the silica in the column.

First hexane and Ethyl acetate (1:1) mixture of 50 ml was poured over the sample followed by adding 50 ml of pure ethyl acetate solvent. Thereafter, fractions of 2 ml were collected in 2ml Eppendorf tubes. The collected samples from almost 38 tubes were analysed using through TLC to check for the presence of BHMF. Pure Ethyl acetate was used as solvent for the TLC.

Gene Identification

2.1.9. Gene Amplification

Given that we are working with a novel bacterium and the specific enzyme involved in the reduction process is unknown, a bioinformatics analysis was conducted. The Candida magnoliae crs1 gene for carbonyl reductase S1 (750 bp) was aligned against *Mycobacterium* MS1601 using BLASTx tool at NCBI **(Appendix Gene Sequence).** A specific sequence was identified, and primers were designed using SnapGene (Dotmatics, Boston, USA), incorporating XhoI and NdeI restriction sites **(Refer to Appendix Table A**. This analysis identified a potential dehydrogenase enzyme that may be present in *Mycobacterium* MS1601 and responsible for the reduction of HMF to BHMF. First, *Mycobacterium* MS1601 was grown in activated media, and the cells were harvested. A DNA extraction kit was then used to extract the DNA.

The gene was then amplified via PCR from *Mycobacterium* MS1601 **(Refer to Appendix Gene sequence)** for detailed PCR conditions). DMSO was also added to the sample for PCR. Three samples were prepared for PCR: one with no DMSO, one with 1.5 µl of DMSO, and the third with 3 µl of DMSO. The PCR product was analysed through gel electrophoresis (1% agarose gel, 71V for 40 minutes) using a PowerPac Basic system (Bio-Rad, USA). DNA concentration was measured with a NanoDrop spectrophotometer (BioSpec-nano, Shimadzu Biotech, Kyoto, Japan).

2.1.10. Digestion and Ligation

The amplified gene sequence was then purified using a Thermo Scientific GeneJET Genomic DNA Purification Kit and subjected to digestion with XhoI and NdeI restriction enzymes, along with the purified pET-28a(+) plasmid following standard protocol by Therofisher for each enzyme **(Appendix Table C).**
Then Ligation reaction was prepared following NEB Ligation Protocol **(Appendix Table D).** The digested products were incubated with T4 DNA ligase (NEB, Massachusetts, USA) at a 1:3 vector/insert ratio. The ligation reaction was carried out for one hour at room temperature. NEBioCalculator was used to calculate molar ratios of insert and vector.

2.1.11. Transformation

About 5µLof cloned plasmid were transformed into 50 µl of *E. coli* DH5α competent cells (Sigma). The mixture was mixed with pipette and incubated on ice for 30 minutes, followed by a heat-shock at 42°C for 30 seconds. After the heat-shock, the mixture was placed back on ice for 2 minutes to recover. Subsequently, 950 µl of pre-warmed SOC medium was added, and the culture was incubated at 220 rpm for 1 hour at 37°C. The cultures were then centrifuged at 1,200 rpm for 1 minute, with 400 µl of the supernatant removed to concentrate the cells. Aliquots of 100 µl and 300 µl of the cell suspension were plated on LB agar plates containing 50 µg/ml kanamycin and incubated overnight at 37°C.

To verify the transformants containing the correct constructs, colony PCR was conducted using T7 forward and reverse primers and DreamTaq Green PCR Master Mix (2X) (Thermoscientific, USA). The PCR products were then analysed by DNA gel electrophoresis to confirm the presence of the target fragments. The PCR conditions are detailed in **Appendix Table.** The plasmids that were correctly cloned for each construct were purified from transformed E. coli DH5α competent cells using the GeneJET Plasmid Miniprep Kit (ThermoScientific, USA). The DNA concentration of the purified plasmids was measured using a NanoDrop (BioSpec-nano, Shimadzu Biotech, Kyoto, Japan).

3. Results and Discussion

Mycobacterium MS1601 reduction reactions

3.1.1. Incubation time and carbon source screening

Activated Media at 24 hours incubation

Figure 1A indicates the effect of glucose as carbon source, where 15 % conversion of HMF was achieved after 24 hours, showing efficient conversion. BHMF production increased steadily, reaching 63.2% at 24 hours, with relatively low HMFCA production (11.1% at 24 hours). Significant BHMF production (62.3%) was observed at 9 hours, indicating efficient conversion within a relatively short time frame. For sorbitol (Figure 1B), 97.4% HMF converted to 54.1% BHMF and 15.5% HMFCA over 24 hours. BHMF production was slightly lower compared to glucose, but HMFCA production was higher. BHMF production reached 53.0% at 9 hours, suggesting good time efficiency but slightly lower selectivity compared to glucose. With glycerol **(Figure 1C)** 60.3% HMF converted to 31.3% BHMF with HMFCA peaking at 19.5% at 24 hours. Among the three carbon sources tested, glucose demonstrated the highest BHMF production and rapid conversion within 9 hours with lower HMFCA levels compared to sorbitol and glycerol.

Activated Media at 48 hours incubation

Glucose **(Figure 1D)** showed significant results in BHMF production, reaching 54.1% at 24 hours. The HMFCA levels increased to 17 %, with total HMF conversion of 72.4 %. For sorbitol (**Figure 1E),** 31.2 % HMF converted to 27.2% BHMF and 3.5% HMFCA. Sorbitol demonstrated low efficiency in converting HMF to BHMF and HMFCA compared to the other carbon sources. With glycerol **(Figure 1F)** BHMF reached 26.7%, HMFCA levels increased to 8.2%, with total HMF conversion of 34.6%. Among the carbon sources, glucose exhibited the highest BHMF production at 54.1%, indicating its effectiveness in BHMF production under these conditions. Glycerol, while showing significant HMFCA production compared to sorbitol, was less effective in BHMF production. Sorbitol was the least effective for this bioconversion process, with the lowest BHMF and HMFCA production. Comparing the 24-hour and 48-hour incubation periods, glucose showed a higher BHMF production at 24 hours (62.3%) compared to 48 hours (54.1%), with a longer incubation leading to increased HMFCA production and more oxidation over time. Sorbitol's efficiency significantly decreased with extended incubation, with BHMF production higher at 24 hours (53.0%) compared to 48 hours (27.2%). Glycerol's BHMF production was highest at 24 hours (68.7%) and decreased to 26.7% at 48 hours, indicating a clear reduction in efficiency with longer incubation.

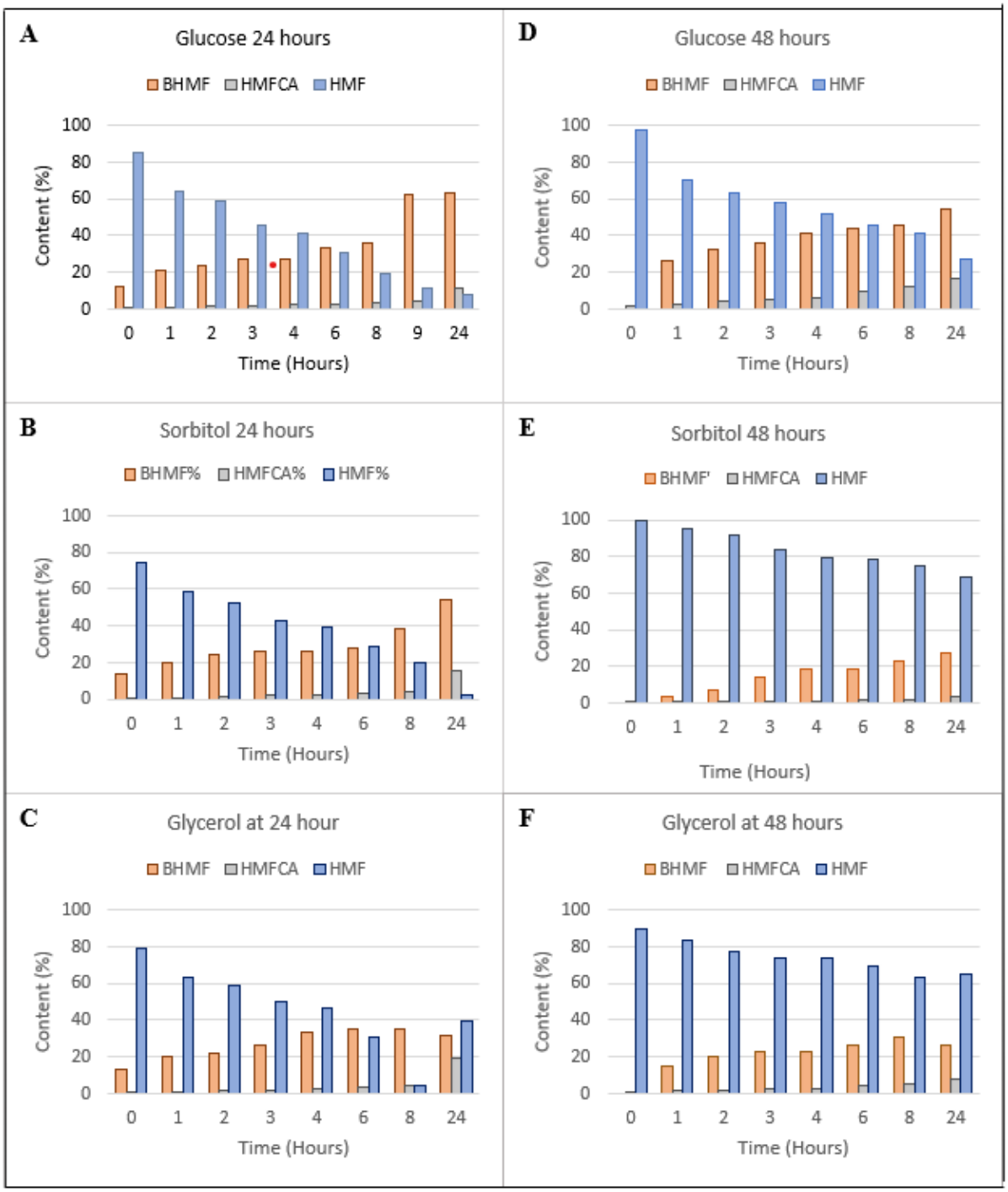

Figure 1: *Cells activated with glucose, sorbitol and glycerol for 24 (A, B, C) and 48 (D, E, F) hours.*

The superior performance of glucose as a carbon source in achieving the highest BHMF yield, compared to glycerol and sorbitol, may be linked to its interaction with glucose dehydrogenase (GDH), which could be the enzyme responsible for reducing HMF to BHMF in our cells. Evidence from studies on *Bacillus subtilis* GDH shows effective NADH regeneration with glucose, which is crucial for this reduction process. In contrast, glycerol and sorbitol enter metabolism less directly and are less efficient in generating NADH, leading to lower BHMF yields (Kornecki et al., 2023). Glucose is also generally the preferred carbon source for microorganisms because it is easily metabolized through glycolysis, providing quick and efficient energy. Bacteria prioritize glucose due to its straightforward entry into central metabolic pathways, enabling rapid growth and energy production. In contrast, sorbitol and glycerol are metabolized less directly and may not supply energy as efficiently. When glucose is scarce, microorganisms increase the production of mRNAs related to carbohydrate transport, enhancing their ability to uptake and utilize other available carbohydrates, thereby adapting to low glucose conditions (Libretexts, 2021).
We also observe that cells incubated for 24 hours show higher efficiency in BHMF production. As seen in **Figure 8,** the cells enter the exponential growth phase around 10 hours, with the optical density (OD) continuing to increase exponentially until approximately 32 hours. This suggests that during this period, the cells are most active, which likely enhances the efficiency of the reduction process from HMF to BHMF. The active metabolism during this growth phase supports optimal enzyme activity for the conversion.

3.1.2. pH screening

To optimize the bioconversion of HMF to BHMF, reactions were tested at pH levels of 6, 7, and 8. At pH 7 **(Figure 2B**), the process demonstrated high efficiency, with 61.1 % BHMF produced and only 8% HMF unconverted after 24 hours. In contrast, at pH 6 **(Figure 2A)**, 32% HMF remained after 24 hours with 46.4% BHMF produced. At pH 8 **(Figure 2C)**, efficiency dropped further, with 59.6% unconverted HMF and only 36% BHMF. These results highlight pH 7 as the optimal condition for rapid and selective bioconversion of HMF to BHMF.

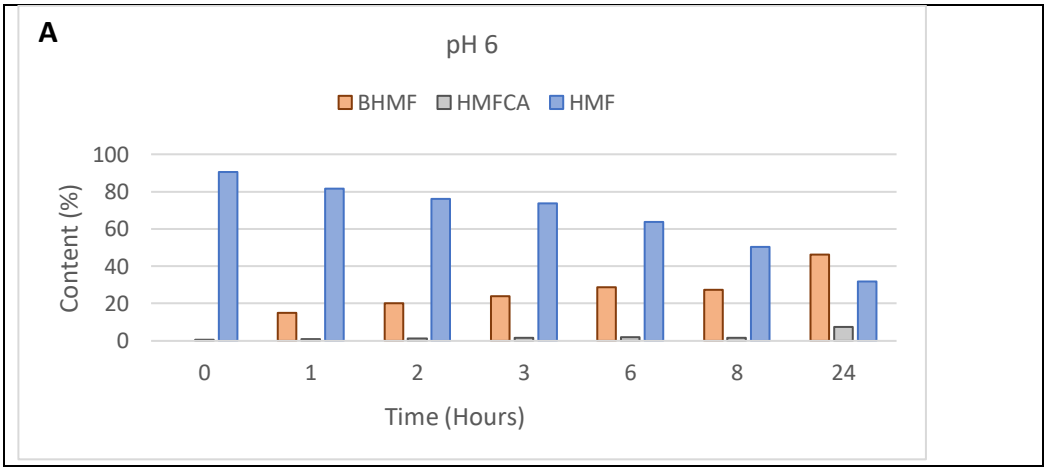

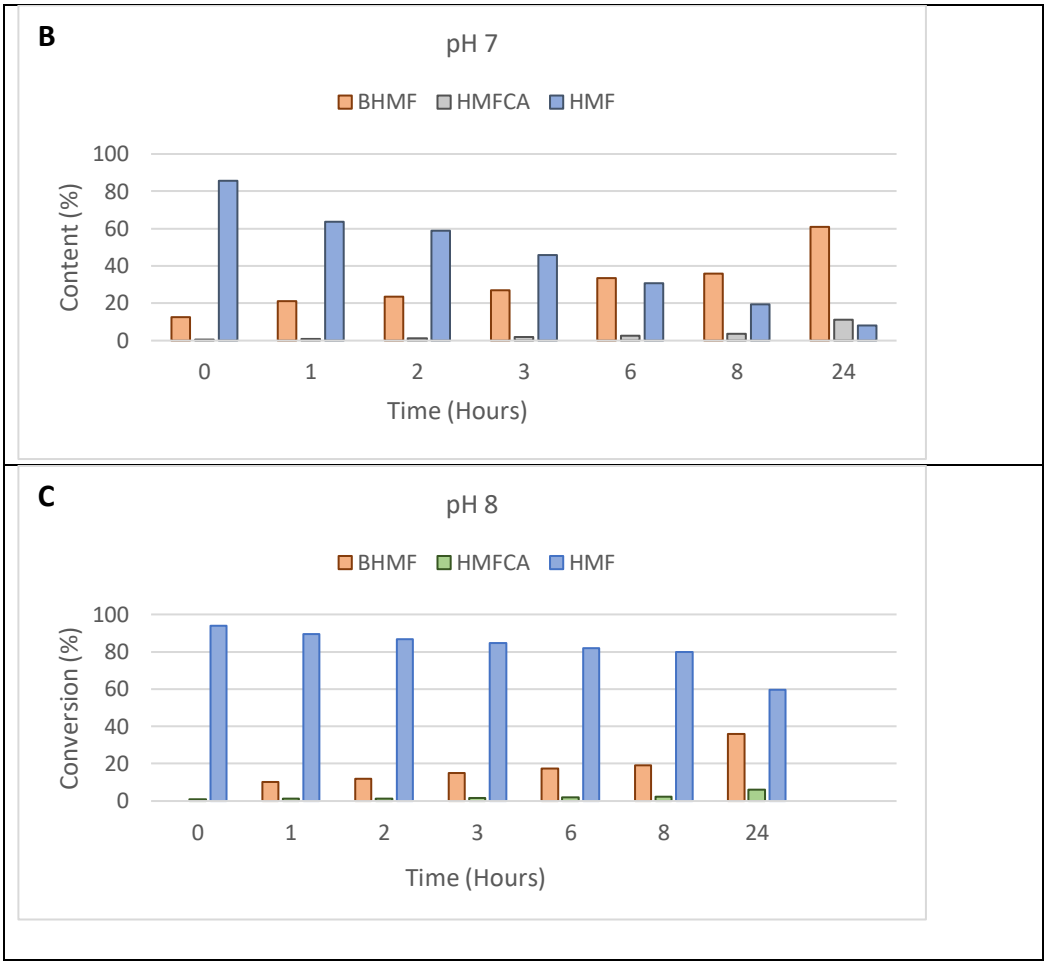

Figure 2: *Percentage yield conversion of HMF to BHMF and HMFCA at pH 6 (2A), 7 (2B) and 8 (2C).*

Based on our previous experiments, glucose proved to be the most effective carbon source for the bioconversion of HMF to BHMF, compared to glycerol and sorbitol. This observation leads to the assumption that glucose dehydrogenase may be playing a key role in the process. Studies involving glucose dehydrogenase in the conversion of HMF to BHMF have demonstrated that pH 7 is the optimal condition for this reaction. At this pH, the enzyme exhibits its highest activity, leading to improved BHMF yields (Kornecki et al., 2023).

3.1.2. NADH supplementation

In the presence of NADH, the BHMF production increased more gradually and did not reach the high levels observed in the control. The control showed a sharp increase upto 62.3% BHMF by 24 hours, compared to 33.9% in the NADH-supplemented reaction **(Figure 3)**. The NADH-supplemented reaction exhibited a higher rate of HMFCA formation early in the reaction but stabilized towards the end. The control, on the other hand, showed a more consistent increase in HMFCA percentage over time. The control was more effective in reducing the residual HMF, dropping to 8% by 24 hours compared to 49.4% in the NADH reaction.
The addition of NADH did not result in the anticipated enhancement of BHMF production. Instead, it slowed the bioconversion process, decreased the efficiency of HMF conversion, and increased the side production of HMFCA. Based on these findings, it is clear that the control conditions (without NADH) provided a better outcome for the production of BHMF.

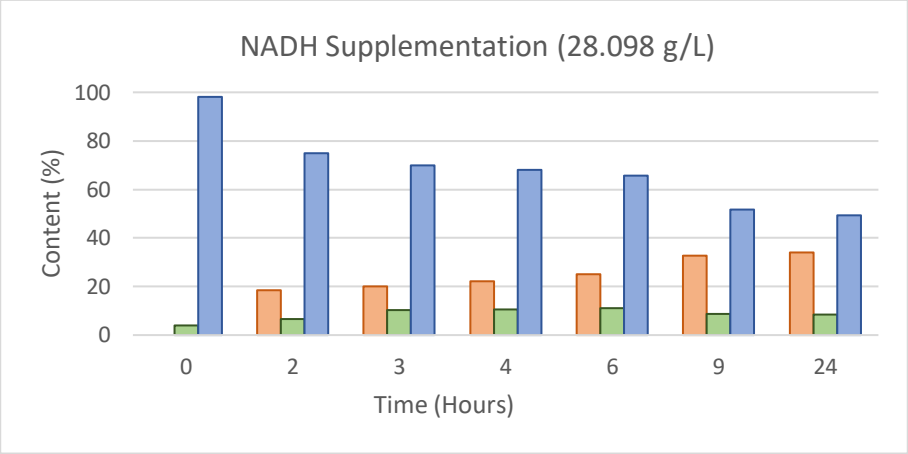

Figure 3: *Percentage yield conversion of HMF to BHMF and HMFCA at pH 8.*

Speculated reasons for NADH not working could be that NADH might have interfered with the enzymatic mechanisms responsible for HMF conversion, potentially by altering enzyme dynamics or by facilitating side reactions that do not lead to BHMF. Adding NADH could disrupt the redox balance within the cells, affecting not only the desired pathways but also enhancing alternative pathways leading to by-products (Yan et al., 2016). The lack of improvement with added NADH may also suggests that other reducing agents or factors might be at play in the reduction of HMF to BHMF. Exploring the roles of NADPH, GSH, and other cellular redox cofactors through assays, as well as optimizing environmental conditions, could help identify more effective strategies for enhancing the yield and selectivity of BHMF production.

3.1.3. Cell concentration screening

Figure 4 shows, two experiments using different concentration of cells 50 gcwd/L and 100 gcwd/L cells respectively, and their effect on BHMF yield. At 50 gcwd/L cells **(Figure 4A),** there was a notably rapid and efficient conversion of HMF to BHMF, achieving a peak BHMF concentration of 80.8% by 6 hours and complete HMF depletion by 4 hours. This suggests that a higher cell density can enhance enzyme availability or activity, thereby accelerating the conversion process. Moreover, the increase in HMFCA formation at this concentration indicates that while the primary conversion pathway to BHMF is enhanced, side reactions leading to by-product formation are also more pronounced, possibly due to the availability of additional enzymes that catalyse alternative pathways or due to metabolic adjustments in denser cultures. In contrast, the experiments with 100 g/L cells **(Figure 4B)** did not yield better results compared to 50 g/L. Despite the rapid depletion of HMF, the maximum BHMF production was only 52.3%, suggesting potential inhibitory effects at this higher cell density. Such inhibitory effects could be due to factors like limited substrate accessibility per cell, diffusion limitations within the dense cell mass, or the accumulation of metabolic by-products that could interfere with enzyme function or cell viability (Riesenberg & Guthke, 1999).

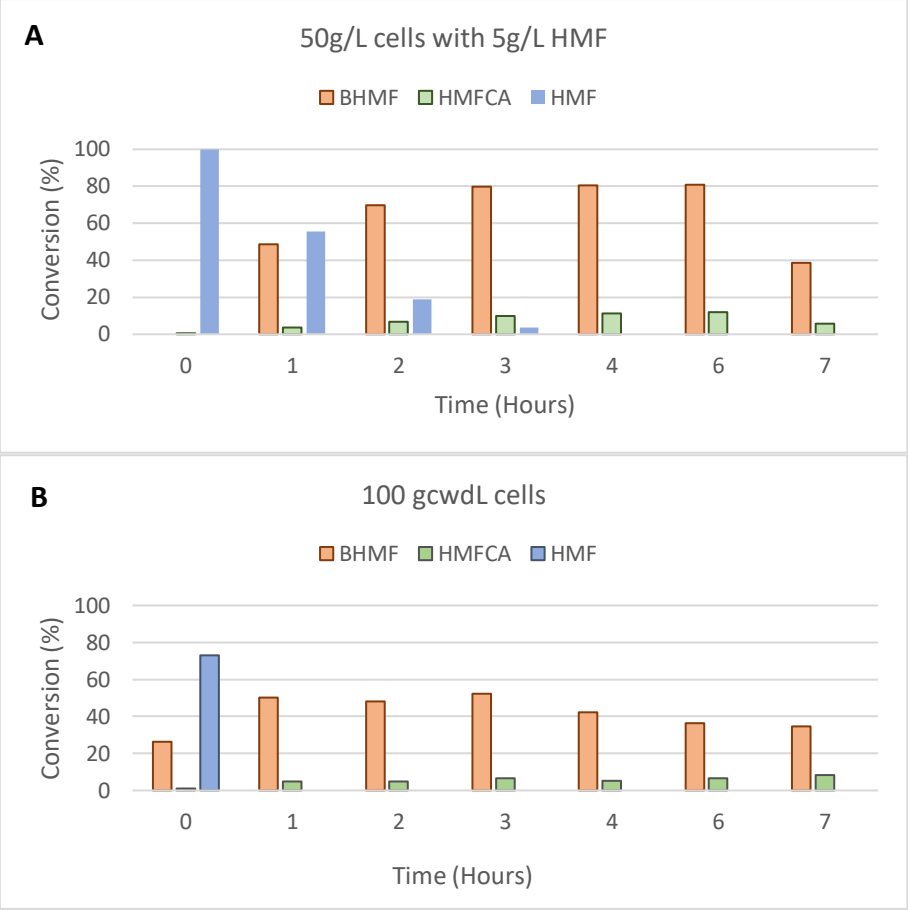

Figure 4: *Percentage yield conversion of 5g/L HMF to BHMF and HMFCA using 50 gcwd/L (A) and 100 gcwd/L (B) cells.*

Comparing these findings with experiment using 20 g/L cells, which achieved a peak BHMF production of about 60% after 24 hours, it is evident that cell density plays a crucial role in dictating the dynamics and outcome of the bioconversion process. While lower cell densities exhibit slower kinetics, they eventually reach substantial BHMF concentrations without the rapid escalation in by-product formation observed at higher densities (Riesenberg & Guthke, 1999).

The optimal cell concentration for this specific bioconversion appears to be 50 g/L, offering a balance between fast conversion rates and high yields of BHMF, while keeping the formation of undesired by-products like HMFCA within manageable levels. These observations underscore the necessity to carefully optimize cell densities in biotransformation processes, considering not only the desired product yield but also the overall reaction efficiency and selectivity (Riesenberg & Guthke, 1999).

3.1.4. Substrate concentration screening

Figure 5A-D show the effect of different HMF concentration (10-25 g/L, respectively) on the reduction rate of HMF into BHMF using the resting cell of *Mycobacterium* sp. 1601. **Figure 5A** indicate the efficient conversion of 92% of HMF within 1h reaction. However, the reduction

rate was decreased to become 37, 31, and 14% of HMF within the same reaction time when HMF concentration was increased to 15, 20, and 25 g/L, respectively **(Figure 5B-D)**. Even though, increasing the substrate conc. of HMF above 10 g/L reduce the reduction rate, the full conversion, 100% as well as a conversion of 67 % have been achieved after 24h with 15 and 20 g/L HMF respectively **(Figure 5B & C).** On the other hand, significant reduction of the conversion rate (only 32%) has been seen with using 25 g/L HMF **(Figure 12 D)**. These findings explain the inhibitory concentration of HMF on the cell activity. Where, no effect of HMF till 10 g/L. Moreover, *Mycobacterium* sp. can overcome the inhibitory effect of HMF at 15 and 20 g/L over long reaction time. It is well known from previous literatures that furan derivatives and phenolic compounds have an inhibitory effect of many microorganisms at very low concertation (Lin et al., 2015). interestingly, *Mycobacterium* sp that used in this study show resistance to higher concentration of HMF highlighting its potential as biocatalyst for biotransformation of HMF into other valuable derivatives

As we know from our previous experiment**,** at the lowest concentration of 5 g/L HMF, there was a high production of BHMF, peaking at 80.81%, with complete HMF conversion by 4 hours. The increase in HMFCA was incremental, peaking later in the process, which suggests high enzymatic efficiency at lower substrate concentrations. As the substrate concentration increased to 10 g/L, BHMF production slowed, reaching 54.7% after 24 hours, and HMFCA significantly increased to 42.8%. This suggests enhanced side reaction activity at slightly higher substrate concentrations, with slower HMF depletion compared to 5 g/L.

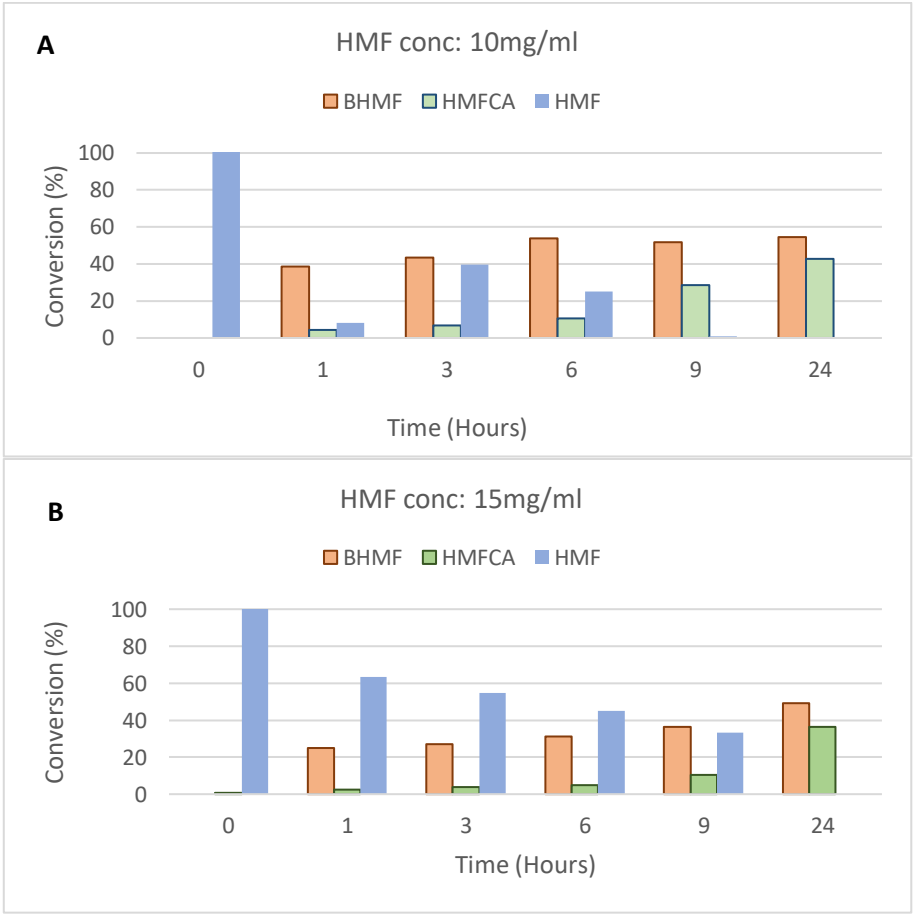

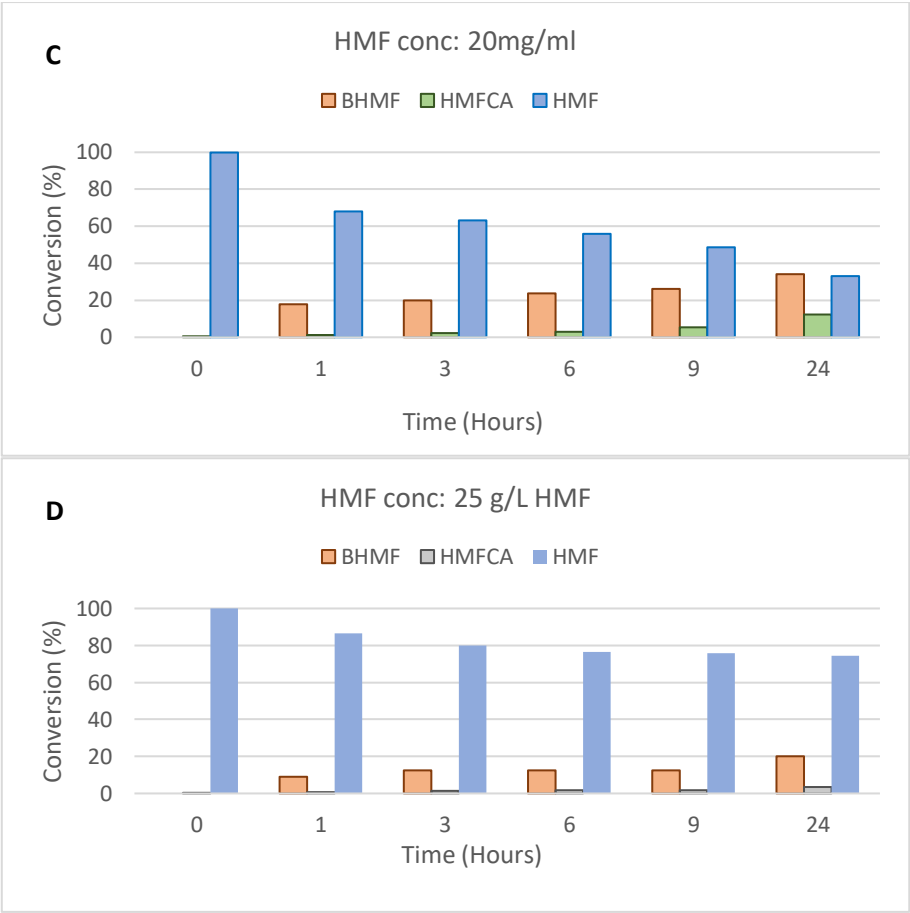

***Figure 5**: Percentage yield conversion of 10-25 g/L HMF (A-D) to BHMF and HMFCA using 50 gcwd/L cells.*

The collected data reveal a clear trend: as the substrate concentration increases, the efficiency of BHMF production decreases while the formation of HMFCA generally increases. This suggests a shift towards side reactions or inhibitory effects impacting the primary conversion pathway. The optimal substrate concentration for maximizing BHMF production with minimal by-product formation appears to be at the lower end of the tested range. This finding is crucial for scaling up the process, suggesting that maintaining lower substrate concentrations might enhance the overall yield and purity of BHMF in industrial applications.

3.1.5. Anaerobic Reaction

The rationale behind using anaerobic conditions stems from the nature of the reactions involved: BHMF production is typically a reduction reaction, whereas HMFCA production is associated with oxidation processes. Thus, eliminating oxygen was hypothesized to potentially suppress the oxidative pathways leading to HMFCA and favor the reduction pathway towards BHMF (Reineke, 2005). Under anaerobic conditions BHMF production increased to 30.8% by 6 hours and eventually reached 48.6% by 24 hours, alongside an increase in HMFCA to 18.8% **(Figure 6)**. Conversely, the control (aerobic) conditions showed a more rapid initial increase in BHMF, reaching 51 % by 6 hours, and culminating at 54.7% by 24 hours. HMFCA production was also higher under aerobic conditions, starting at zero and escalating to 42.8% by the end of the experiment.

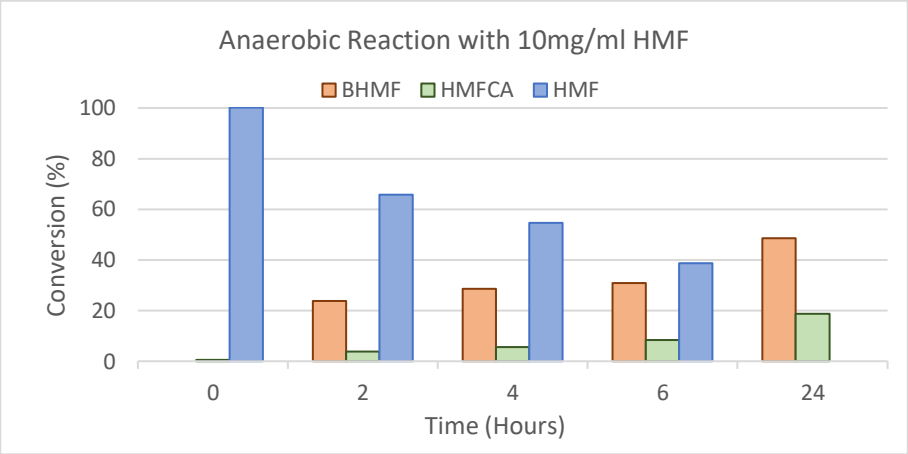

Figure 6: Percentage yield conversion of 10 g/L HMF to BHMF and HMFCA using 50 g/L cells under anaerobic condition.

The analysis reveals that aerobic conditions accelerate the formation of BHMF earlier in the reaction, potentially due to enhanced enzymatic activities that utilize oxygen either directly or indirectly. Both conditions achieved complete consumption of HMF by the 24-hour mark, but the kinetics of this process differed markedly. As expected, the aerobic (control) reaction shows a much higher level of HMFCA, indicating that oxidative processes are more pronounced in the presence of oxygen. However, the fact that HMFCA is still produced under anaerobic conditions implies that some oxidation pathways are still active, possibly due to residual oxygen or other oxidative mechanisms (Naifeh et al., 2023).

In conclusion, HMFCA production in anaerobic condition might suggest that under anaerobic conditions, cells might use alternative electron acceptors or redox couples to drive the reduction of HMF to BHMF (Shan et al., 2012). These alternative pathways could still lead to the formation of HMFCA, albeit at a lower rate. The differences in final BHMF concentrations between the two conditions are relatively minor, highlighting those factors such as enzyme availability or the presence of co-factors may also play significant roles

3.1.6. Upscale Bioreactor Reaction

In the bioreactor, BHMF production reached 63.0 g/L after 24 hours, while in the shake flask, it only reached 34.27 g/L, illustrating the improved efficiency of the bioreactor **(Figure 7)**. Despite this increased BHMF production, the by-product HMFCA concentrations remained similar between the two systems, with levels of 12.45 g/L in the shake flask (10 ml reaction) and 12.7 g/L in the bioreactor, suggesting that the scale-up or improved aeration did not significantly impact oxidative side reactions. The comparable residual HMF concentrations in both systems (32.97 g/L in the shake flask vs. 33.4 g/L in the bioreactor) indicate that the shake flask may have experienced more side reactions, leading to the formation of other HMF derivatives, while the bioreactor's controlled environment minimized these pathways and allowed for more efficient HMF conversion to BHMF.

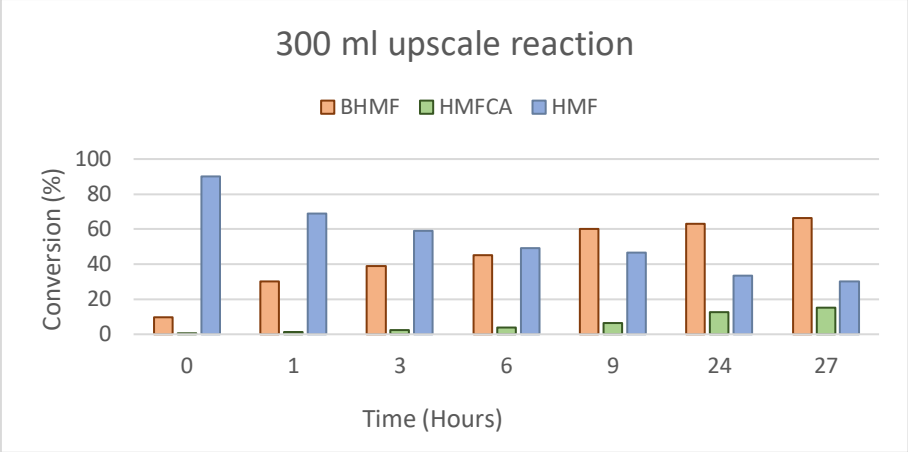

Figure 7: Percentage yield conversion of 20 g/L HMF to BHMF and HMFCA using 37 g/L cells.

The higher enzyme efficiency observed in the bioreactor is likely due to several factors. First, the tight control of oxygen levels is critical, as it helps maintain redox balance, which is essential for enzymes involved in the reduction of HMF. The oxygen transfer rate in the bioreactor was optimized, preventing oxygen limitation that might have occurred in the shake flask due to less efficient aeration and mixing. Second, the bioreactor's ability to maintain constant pH (7) and temperature (30°C) ensured that the enzymes were operating under optimal conditions for the entire duration of the reaction. Deviations in pH and temperature, which are more likely in shake flasks, can negatively impact enzyme activity and stability, leading to the formation of undesired by-products (Raza et al., 2019).
Furthermore, the higher cell density and more efficient mixing in the bioreactor contributed to the faster reaction kinetics. In the shake flask, substrate gradients and limited oxygen availability could have led to localized regions of enzyme inhibition or substrate depletion, reducing overall BHMF production. In contrast, the bioreactor's larger working volume and better-controlled gas exchange promoted a more stable environment, allowing for faster substrate conversion and higher BHMF yield (Ganjave et al., 2022).

3.1.7. OD vs Time

From 0 to 6 hours, the cells are in the Lag Phase, during which the optical density (OD) changes slowly from 0.247 to 0.294, indicating that the cells are acclimating to their new environment (Figure 8). From 6 to 32 hours, the cells enter the Exponential (Log) Phase, where they undergo rapid and continuous growth, as evidenced by the increase in OD from 0.294 to 4.166. The steady rise in OD without a clear plateau suggests that the cells remain in the exponential growth phase throughout this period.

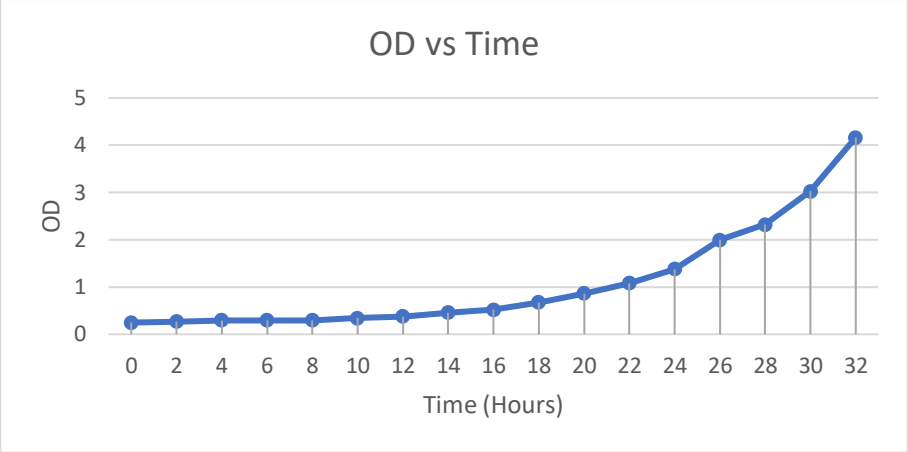

Figure 8: OD vs Time graph

Extraction and Purification of BHMF

3.1.8. Flash Column Chromatography

After performing liquid-liquid extraction using reaction sample, we successfully extracted BHMF Glaser et al. (2023); however, traces of HMFCA were still present **(Refer to S1 in Figure 10).** To further purify the extract, we conducted flash chromatography (Saikia et al., 2021). Once the process was complete and the eluents were collected in tubes, we randomly selected vials, skipping every second Eppendorf tube. From each selected tube, we took approximately 2 µl of sample and applied it to a TLC plate along with standards BHMF, HMF, and HMFCA. The TLC plate, treated with p-Anisaldehyde stain, is shown in **Figure 9A** below. The presence of BHMF was observed in the sample from the 29th tube. Additionally, samples from tubes 28 to 31 were tested, revealing the fraction containing our purified BHMF **(Figure 9B).**

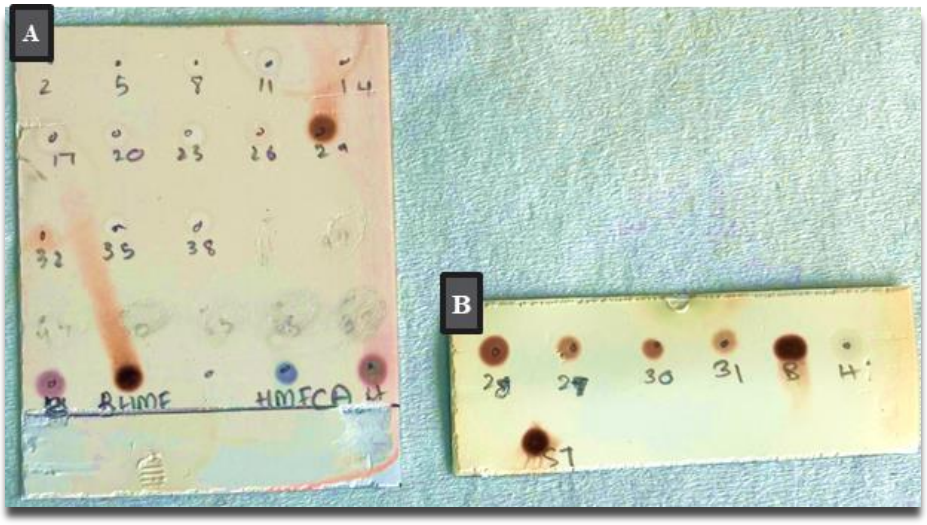

Figure 9: Preliminary TLC Analysis for Detection of BHMF Presence.

To further confirm, we ran a proper TLC in ethyl acetate as the mobile phase **(Figure 10)**. It was observed that unlike S1 (un-purified sample) none of the purified samples (27-31) contained HMF or HMFCA and that sample were in fact pure BHMF. These tubes were then combined and completely dried for NMR analysis

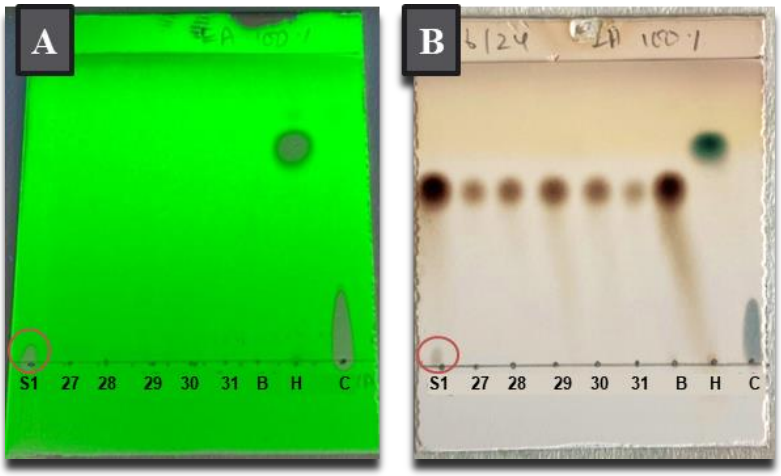

Figure 10: TLC plates under UV light 254nm (left image) and after developing (right image) with standards BHMF (B), HMF (H), and HMFCA (C).

The initial concentration of BHMF in the raw sample was approximately 7 g/L. After the liquid-liquid extraction and subsequent purification via column chromatography, we successfully purified 3 grams of the product. While the process demonstrated success, the yield indicates a significant product loss during purification. This suggests that there is considerable room for improvement in the efficiency of the extraction and purification steps. Optimizing these processes could help reduce product loss and improve overall yield, potentially enhancing both the efficiency and cost-effectiveness of the method.

3.1.2. NMR

In the NMR spectrum obtained for BHMF (**Figure 11)**, distinct peaks were observed, which correspond to the protons present in the molecule's structure. The solvent peak indicates the chloroform used during the analysis.

Two main signals, labeled as 1 and 2, correspond to the distinct proton environments in BHMF. Signal 1 appears at approximately at 6.27ppm for the protons adjacent to the furan ring, while Signal 2 at 4.62 ppm represents the hydroxymethyl proton group. The intensity and splitting patterns of these peaks align with the expected structure of BHMF, confirming its identity. The clear separation of these peaks suggests the purity of the sample and the effectiveness of the synthesis process.

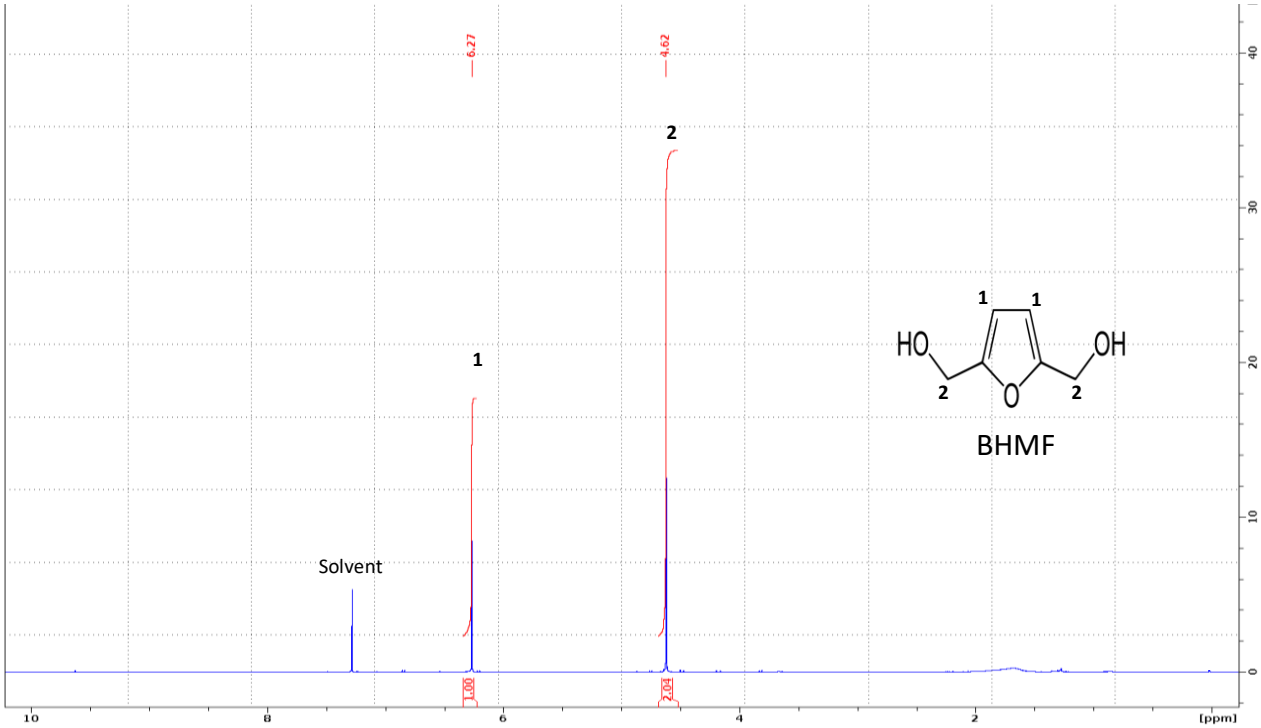

Figure 11: BHMF NMR spectra (Chloroform): δ 6.27, and 4.62 belong to 2,5- bishydroxymethylfuran (BHMF).

Molecular Analysis

3.1.3. Amplification and Gel Electrophoresis

The *Candida magnoliae* crs1 gene showed a successful match against the sequence for glucose 1-dehydrogenase *Mycobacterium* sp. MS1601, with a sequence identity of 30.83%, indicating a reasonable level of similarity **(Figure 12)**.

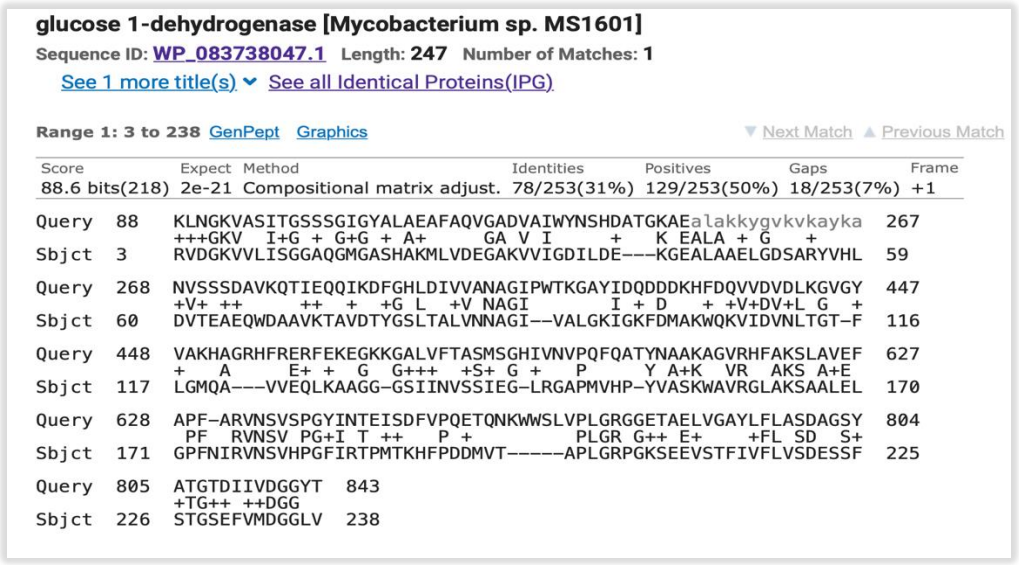

Figure 12: Blast results showing alignment between Candida magnoliae crs1 gene and glucose 1-dehydrogenase [Mycobacterium sp. MS1601].

Primers were then designed for the glucose 1-dehydrogenase gene to amplify the gene sequence from the extracted and purified *Mycobacterium* sp. MS1601 DNA. Given that the gene length was 750 bp, clear bands were observed at approximately 750 bp for all three samples, as shown in **Figure 13**.

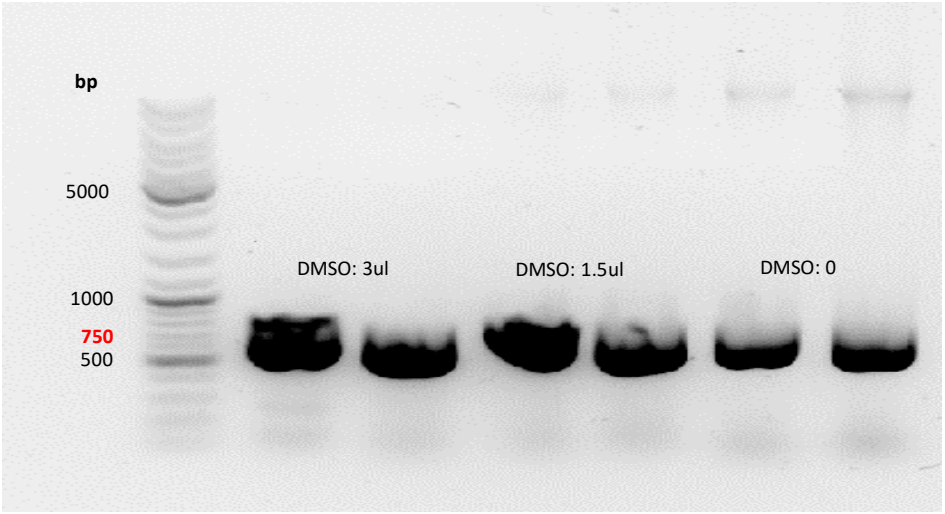

Figure 13: *Gel Electrophoresis showing amplified target Mycobacterium sp. MS1601 DNA.*

3.1.4. Cloning and Transformation

After screening numerous colonies, two colonies yielded positive results. Both displayed a band around 750 bp, indicating the successful insertion of our gene into the plasmid **(Figure 14)**.

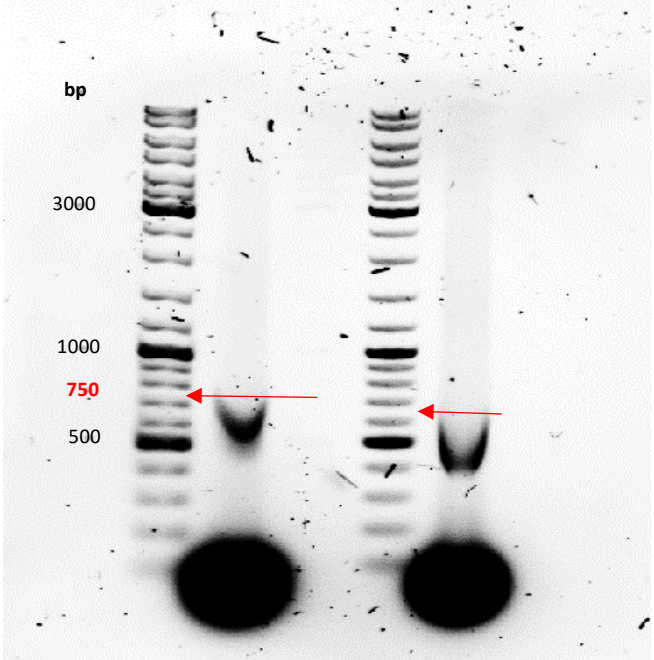

***Figure 14**: Verification of successful transformation of insert in BL28 plasmid via gel electrophoresis.*

Conclusion

This study successfully demonstrated the bioconversion of HMF to BHMF using *Mycobacterium* MS1601, achieving an 80% BHMF yield within 4 hours and complete conversion of HMF by optimizing parameters such as a 24-hour incubation duration, glucose as the carbon source, pH 7, and a cell concentration of 50 g/L. The identification, amplification, and cloning of the glucose 1-dehydrogenase gene were confirmed by clear 750 bp bands in PCR, and the extraction and purification process yielded high-purity BHMF, as confirmed by TLC.

Future work should focus on exploring fed-batch reactors by gradually increasing HMF concentrations to acclimate the cells and enhance yields. Additionally, expressing and purifying the glucose 1-dehydrogenase protein in suitable expression systems, and testing its ability to reduce HMF to BHMF, followed by conducting enzymatic assays to characterize the enzyme, and performing structural studies will provide insights into its catalytic mechanism and potential for engineering. Exploring the use of different co-factors or co-factor regeneration systems will maintain high levels of active co-factors during the bioconversion process, enhancing enzyme activity. Implementing in situ product recovery (ISPR) techniques can continuously remove BHMF from the reaction mixture, preventing product inhibition and improving overall yields. Experimenting with different medium compositions may also help find the optimal nutrient balance for maximum BHMF production. Larger-scale bioreactor experiments and investigating alternative methods for BHMF extraction and purification, beyond liquid-liquid extraction, will further improve yields and efficiency, paving the way for scalable industrial applications.

References

Alamillo, R., Tucker, M., Chia, M., Pagán-Torres, Y., & Dumesic, J. (2012). The selective hydrogenation of biomass-derived 5-hydroxymethylfurfural using heterogeneous catalysts. *Green Chemistry*, *14*(5), 1413. https://doi.org/10.1039/c2gc35039d

Baptista, M., Cunha, J. T., & Domingues, L. (2021). Establishment of Kluyveromyces marxianus as a Microbial Cell Factory for Lignocellulosic Processes: Production of High Value Furan Derivatives. *Journal of Fungi*, *7*(12), 1047. https://doi.org/10.3390/jof7121047

Chang, S., He, X., Li, B., & Pan, X. (2021). Improved Bio-Synthesis of 2,5-bis(hydroxymethyl)furan by Burkholderia contaminans NJPI-15 With Co-substrate. *Frontiers in Chemistry*, *9*. https://doi.org/10.3389/fchem.2021.635191

Chatterjee, M., Ishizaka, T., & Kawanami, H. (2014). Selective hydrogenation of 5-hydroxymethylfurfural to 2,5-bis-(hydroxymethyl)furan using Pt/MCM-41 in an aqueous medium: a simple approach. *Green Chemistry*, *16*(11), 4734–4739. https://doi.org/10.1039/c4gc01127a

Chen, D., Cang, R., Zhang, Z., Huang, H., Zhang, Z., & Ji, X. (2021). Efficient reduction of 5-hydroxymethylfurfural to 2, 5-bis (hydroxymethyl) furan by a fungal whole-cell biocatalyst. *Molecular Catalysis*, *500*, 111341. https://doi.org/10.1016/j.mcat.2020.111341

Cunha, J. T., Romaní, A., & Domingues, L. (2022). Whole cell biocatalysis of 5-Hydroxymethylfurfural for sustainable biorefineries. *Catalysts*, *12*(2), 202. https://doi.org/10.3390/catal12020202

Davidson, M. G., Elgie, S., Parsons, S., & Young, T. J. (2021). Production of HMF, FDCA and their derived products: a review of life cycle assessment (LCA) and techno-economic analysis (TEA) studies. *Green Chemistry*, *23*(9), 3154–3171. https://doi.org/10.1039/d1gc00721a

De Luna, G. S., Ho, P. H., Sacco, A., Hernández, S., Velasco-Vélez, J., Ospitali, F., Paglianti, A., Albonetti, S., Fornasari, G., & Benito, P. (2021). AGCU Bimetallic electrocatalysts for the reduction of Biomass-Derived compounds. *ACS Applied Materials & Interfaces*, *13*(20), 23675–23688. https://doi.org/10.1021/acsami.1c02896

Demirbas, A. (2009). Combustion efficiency impacts of biofuels. *Energy Sources Part a Recovery Utilization and Environmental Effects*, *31*(7), 602–609. https://doi.org/10.1080/15567030701743718

Glaser, S. J., Pyo, S., Rehnberg, N., Rother, D., & Hatti-Kaul, R. (2023). Carboligation of 5-(hydroxymethyl)furfural via whole-cell catalysis to form C12 furan derivatives and their use for hydrazone formation. *Microbial Cell Factories*, *22*(1). https://doi.org/10.1186/s12934-023-02130-1

Guo, Y., & Chen, J. (2016). Photo-induced reduction of biomass-derived 5-hydroxymethylfurfural using graphitic carbon nitride supported metal catalysts. *RSC Advances*, *6*(104), 101968–101973. https://doi.org/10.1039/c6ra19153c

Han, J., Kim, Y., Jang, H., Hwang, S., Jegal, J., Kim, J. W., & Lee, Y. (2016). Heterogeneous zirconia-supported ruthenium catalyst for highly selective hydrogenation of 5-hydroxymethyl-2-furaldehyde to 2,5-bis(hydroxymethyl)furans in various n-alcohol solvents. *RSC Advances*, *6*(96), 93394–93397. https://doi.org/10.1039/c6ra18016g

Hao, C., Guo, X., Pan, Y., Chen, S., Jiao, Z., Yang, H., & Guo, X. (2016a). Visible-Light-Driven Selective Photocatalytic Hydrogenation of Cinnamaldehyde over Au/SiC Catalysts. *Journal of the American Chemical Society*, *138*(30), 9361–9364. https://doi.org/10.1021/jacs.6b04175

Hao, C., Guo, X., Pan, Y., Chen, S., Jiao, Z., Yang, H., & Guo, X. (2016b). Visible-Light-Driven Selective Photocatalytic Hydrogenation of Cinnamaldehyde over Au/SiC Catalysts. *Journal of the American Chemical Society*, *138*(30), 9361–9364. https://doi.org/10.1021/jacs.6b04175

He, Y., Jiang, C., Chong, G., Di, J., & Ma, C. (2018). Biological synthesis of 2,5-bis(hydroxymethyl)furan from biomass-derived 5-hydroxymethylfurfural by E. coli CCZU-K14 whole cells. *Bioresource Technology*, *247*, 1215–1220. https://doi.org/10.1016/j.biortech.2017.09.071

He, Y., Tao, Z., Zhang, X., Yang, Z., & Xu, J. (2014). Highly efficient synthesis of ethyl (S)-4-chloro-3-hydroxybutanoate and its derivatives by a robust NADH-dependent reductase from E. coli CCZU-K14. *Bioresource Technology*, *161*, 461–464. https://doi.org/10.1016/j.biortech.2014.03.133

Howell, B. A., & Lazar, S. T. (2018). Biobased Plasticizers from Carbohydrate-Derived 2,5-Bis(hydroxymethyl)furan. *Industrial & Engineering Chemistry Research*, *58*(3), 1222–1228. https://doi.org/10.1021/acs.iecr.8b05442

Hu, F., La Scala, J. J., Sadler, J. M., & Palmese, G. R. (2016). Correction to synthesis and characterization of thermosetting Furan-Based Epoxy systems. *Macromolecules*, *49*(6), 2408. https://doi.org/10.1021/acs.macromol.5b02801

Hu, L., Dai, X., Li, N., Tang, X., & Jiang, Y. (2019). Highly selective hydrogenation of biomass-derived 5-hydroxymethylfurfural into 2,5-bis(hydroxymethyl)furan over an acid–base bifunctional hafnium-based coordination polymer catalyst. *Sustainable Energy & Fuels*, *3*(4), 1033–1041. https://doi.org/10.1039/c8se00545a

Kinghorn, A. D. (1997). Plant Drug Analysis. A Thin Layer Chromatography Atlas. Second Edition By H. Wagner and S. Bladt (Universität München). Photographs by V. Rickl. Springer-Verlag, Brooklyn, New York. 1996. xv+ 384 pp. 19.5 × 24 cm. "98.00. ISBN 3-540-58676-8. *Journal of Natural Products*, *60*(4), 428. https://doi.org/10.1021/np960627o

Lăcătuş, M. A., Bencze, L. C., Toşa, M. I., Paizs, C., & Irimie, F. (2018). Eco-Friendly Enzymatic Production of 2,5-Bis(hydroxymethyl)furan Fatty Acid Diesters, Potential Biodiesel Additives. *ACS Sustainable Chemistry & Engineering*, *6*(9), 11353–11359. https://doi.org/10.1021/acssuschemeng.8b01206

Li, C., & Na, Y. (2021). Recent advances in photocatalytic oxidation of 5-Hydroxymethylfurfural. *ChemPhotoChem*, *5*(6), 502–511. https://doi.org/10.1002/cptc.202000261

Li, H., He, J., Riisager, A., Saravanamurugan, S., Song, B., & Yang, S. (2016). Acid–Base bifunctional zirconium N-Alkyltriphosphate nanohybrid for hydrogen transfer of Biomass-Derived carboxides. *ACS Catalysis*, *6*(11), 7722–7727. https://doi.org/10.1021/acscatal.6b02431

Li, Y., Zhang, X., Li, N., Xu, P., Lou, W., & Zong, M. (2016a). Biocatalytic Reduction of HMF to 2,5-Bis(hydroxymethyl)furan by HMF-Tolerant Whole Cells. *ChemSusChem*, *10*(2), 372–378. https://doi.org/10.1002/cssc.201601426

Li, Y., Zhang, X., Li, N., Xu, P., Lou, W., & Zong, M. (2016b). Biocatalytic Reduction of HMF to 2,5-Bis(hydroxymethyl)furan by HMF-Tolerant Whole Cells. *ChemSusChem*, *10*(2), 372–378. https://doi.org/10.1002/cssc.201601426

Liu, F., Audemar, M., De Oliveira Vigier, K., Clacens, J., De Campo, F., & François, J. (2014). Combination of Pd/C and Amberlyst-15 in a single reactor for the acid/hydrogenating catalytic conversion of carbohydrates to 5-hydroxy-2,5-hexanedione. *Green Chemistry*, *16*(9), 4110–4114. https://doi.org/10.1039/c4gc01158a

Liu, Z., Huang, Z., Zhao, W., & Liu, X. (2022). Highly efficient Ni–NiO/carbon nanotubes catalysts for the selective transfer hydrogenation of 5-hydroxymethylfurfural to 2,5-bis(hydroxymethyl)furan. *Reaction Chemistry & Engineering*, *7*(8), 1873–1878. https://doi.org/10.1039/d2re00134a

Liu,A, F. L., A., & Audemar, M. (2014). Combination of Pd/C and Amberlyst-15 in a single reactor for the acid/hydrogenating catalytic conversion of carbohydrates to 5-hydroxy-2,5-hexanedione. *Green Chemistry*.

Millán, A., Sala, N., Torres, M., & Canela-Garayoa, R. (2021). Biocatalytic Transformation of 5-Hydroxymethylfurfural into 2,5-di(hydroxymethyl)furan by a Newly Isolated Fusarium striatum Strain. *Catalysts*, *11*(2), 216. https://doi.org/10.3390/catal11020216

Mishra, D. K., Lee, H. J., Truong, C. C., Kim, J., Suh, Y., Baek, J., & Kim, Y. J. (2020). Ru/MnCo2O4 as a catalyst for tunable synthesis of 2,5-bis(hydroxymethyl)furan or 2,5-bis(hydroxymethyl)tetrahydrofuran from hydrogenation of 5-hydroxymethylfurfural. *Molecular Catalysis*, *484*, 110722. https://doi.org/10.1016/j.mcat.2019.110722

Ohyama, J., Hayashi, Y., Ueda, K., Yamamoto, Y., Arai, S., & Satsuma, A. (2016). Effect of FEOX modification of AL2O3 on its supported AU catalyst for hydrogenation of 5-Hydroxymethylfurfural. *The Journal of Physical Chemistry C*, *120*(28), 15129–15136. https://doi.org/10.1021/acs.jpcc.6b01542

Post, C., Maniar, D., Voet, V. S. D., Folkersma, R., & Loos, K. (2023a). Biobased 2,5-Bis(hydroxymethyl)furan as a Versatile Building Block for Sustainable Polymeric Materials. *ACS Omega*, *8*(10), 8991–9003. https://doi.org/10.1021/acsomega.2c07629.

Pyo, S., Sayed, M., & Hatti-Kaul, R. (2019). Batch and Continuous Flow Production of 5-Hydroxymethylfurfural from a High Concentration of Fructose Using an Acidic Ion Exchange Catalyst. Organic Process Research & Development, 23(5), 952–960. https://doi.org/10.1021/acs.oprd.9b00044ayed

S, M., Dishisha, T., Sayed, W. F., Salem, W. M., Temerk, H. M., & Pyo, S. (2017). Enhanced selective oxidation of trimethylolpropane to 2,2-bis(hydroxymethyl)butyric acid using Corynebacterium sp. ATCC 21245. *Process Biochemistry*, *63*, 1–7. https://doi.org/10.1016/j.procbio.2017.08.007

Sayed, M., Gaber, Y., Junghus, F., Martín, E. V., Pyo, S., & Hatti-Kaul, R. (2022). Oxidation of 5-hydroxymethylfurfural with a novel aryl alcohol oxidase from Mycobacterium sp. MS1601. *Microbial Biotechnology*, *15*(8), 2176–2190. https://doi.org/10.1111/1751-7915.14052

Sayed, M., Warlin, N., Hulteberg, C., Munslow, I., Lundmark, S., Pajalic, O., Tunå, P., Zhang, B., Pyo, S., & Hatti-Kaul, R. (2020). 5-Hydroxymethylfurfural from fructose: an efficient continuous process in a water-dimethyl carbonate biphasic system with high yield product recovery. Green Chemistry, 22(16), 5402–5413. https://doi.org/10.1039/d0gc01422b

Stensrud, K., Wicklund, L., & Co, A. D. M. (2014, August 19). *US20170226075A1 - Synthesis of Non-Ionic surfactants from 5-Hydroxymethyl-2-Furfural, Furan-2,5-Dimethanol and Bis-2,5-Dihydroxymethyl-Tetrahydrofurans - Google Patents*. https://patents.google.com/patent/US20170226075A1/en

Vaidyanathan, V. K., Saikia, K., Kumar, P. S., Rathankumar, A. K., Rangasamy, G., & Saratale, G. D. (2023). Advances in enzymatic conversion of biomass derived furfural and 5-hydroxymethylfurfural to value-added chemicals and solvents. *Bioresource Technology*, *378*, 128975. https://doi.org/10.1016/j.biortech.2023.128975

Van Putten, R., Van Der Waal, J. C., De Jong, E., Rasrendra, C. B., Heeres, H. J., & De Vries, J. G. (2013a). Hydroxymethylfurfural, A Versatile Platform Chemical Made from Renewable Resources. *Chemical Reviews*, *113*(3), 1499–1597. https://doi.org/10.1021/cr300182k

Wang, G., Deng, X., Gu, D., Chen, K., Tüysüz, H., Spliethoff, B., Bongard, H., Weidenthaler, C., Schmidt, W., & Schüth, F. (2016). Co3O4 Nanoparticles Supported on Mesoporous Carbon for Selective Transfer Hydrogenation of α,β-Unsaturated Aldehydes. *Angewandte Chemie*, *55*(37), 11101–11105. https://doi.org/10.1002/anie.201604673

Xia, H., Xu, S., Hu, H., An, J., & Li, C. (2018). Efficient conversion of 5-hydroxymethylfurfural to high-value chemicals by chemo- and bio-catalysis. *RSC Advances*, *8*(54), 30875–30886. https://doi.org/10.1039/c8ra05308a

Xia, Z., Zong, M., & Li, N. (2020). Catalytic synthesis of 2,5-bis(hydroxymethyl)furan from 5-hydroxymethylfurfual by recombinant Saccharomyces cerevisiae. *Enzyme and Microbial Technology*, *134*, 109491. https://doi.org/10.1016/j.enzmictec.2019.109491

Xu, J., He, A., Wu, B., Hu, L., Liu, X., Wu, Z., Xia, J., Xu, J., & Zhou, S. (2020). Redox-Switchable Biocatalyst for Controllable Oxidation or Reduction of 5-Hydroxymethylfurfural into High-Value Derivatives. *ACS Omega*, *5*(31), 19625–19632. https://doi.org/10.1021/acsomega.0c02178

Xu, J., Zhu, Z., Yuan, Z., Su, T., Zhao, Y., Ren, W., Zhang, Z., & Lü, H. (2019). Selective oxidation of 5-hydroxymethylfurfural to 5-formyl-2-furancar-boxylic acid over a Fe-Anderson type catalyst. *Journal of the Taiwan Institute of Chemical Engineers*, *104*, 8–15. https://doi.org/10.1016/j.jtice.2019.08.006

Xu, Z., Cheng, A., Xing, X., Zong, M., Bai, Y., & Li, N. (2018). Improved synthesis of 2,5-bis(hydroxymethyl)furan from 5-hydroxymethylfurfural using acclimatized whole cells entrapped in calcium alginate. *Bioresource Technology*, *262*, 177–183. https://doi.org/10.1016/j.biortech.2018.04.077

Zhang, L., Michel, F. C., & Co, A. C. (2019). Nonisocyanate route to 2,5-bis(hydroxymethyl)furan-based polyurethanes crosslinked by reversible diels–alder reactions. *Journal of Polymer Science Part a Polymer Chemistry*, *57*(14), 1495–1499. https://doi.org/10.1002/pola.29418

Zhao, W., Wang, F., Zhao, K., Liu, X., Zhu, X., Yan, L., Yin, Y., Xu, Q., & Yin, D. (2023). Recent advances in the catalytic production of bio-based diol 2,5-bis(hydroxymethyl)furan. *Carbon Resources Conversion*, *6*(2), 116–131. https://doi.org/10.1016/j.crcon.2023.01.001

Zhu, Y., Kong, X., Zheng, H., Ding, G., Zhu, Y., & Li, Y. (2015). Efficient synthesis of 2,5-dihydroxymethylfuran and 2,5-dimethylfuran from 5-hydroxymethylfurfural using mineral-derived Cu catalysts as versatile catalysts. *Catalysis Science & Technology*, *5*(8), 4208–4217. https://doi.org/10.1039/c5cy00700c

Appendix

Gene Sequence

```
>AB036927.1 Candida magnoliae crs1 gene for carbonyl reductase S1, complete
cds
ATGGCTAAGAACTTCTCCAACGTCGAGTACCCCGCCCCGCCTCCGGCCCACACCAAGAACGAGTCGCTGC
AGGTCCTTGACCTGTTCAAGCTGAATGGCAAGGTTGCCAGCATCACTGGCTCGTCCAGCGGTATTGGCTA
CGCTCTGGCTGAGGCCTTCGCGCAGGTCGGCGCTGACGTCGCCATCTGGTACAACAGCCACGACGCTACT
GGCAAGGCTGAGGCCCTCGCCAAGAAGTACGGCGTCAAGGTCAAGGCCTACAAGGCGAACGTGAGCAGCT
CTGACGCCGTGAAGCAGACGATCGAGCAGCAGATCAAGGACTTCGGCCACCTCGACATTGTCGTGGCGAA
CGCCGGCATTCCCTGGACGAAGGGTGCCTACATCGACCAGGACGACGACAAGCACTTCGACCAGGTCGTT
GACGTCGATCTGAAGGGTGTTGGATACGTCGCGAAGCACGCTGGCCGTCACTTCCGCGAGCGCTTCGAGA
AGGAGGGCAAGAAGGGCGCCCTTGTGTTCACGGCCTCCATGTCTGGCCACATTGTGAACGTGCCCCAGTT
CCAGGCCACGTACAACGCGGCCAAGGCTGGCGTGCGCCACTTCGCGAAGTCGCTGGCCGTCGAGTTCGCG
CCGTTCGCGCGCGTGAACTCTGTGTCGCCGGGCTACATCAACACGGAGATCTCGGACTTCGTGCCCCAGG
AGACGCAGAACAAGTGGTGGTCGCTCGTGCCCCTTGGCCGCGGCGGAGAGACGGCCGAGCTCGTTGGCGC
CTACCTGTTCCTTGCATCTGACGCCGGCTCGTACGCCACTGGTACGGACATCATTGTTGACGGTGGCTAC
ACGCTTCCCTAA
```

Reference
Yu-Cai He, Zhi-Cheng Tao, Xian Zhang, Zhen-Xing Yang, Jian-He Xu,
Highly efficient synthesis of ethyl (S)-4-chloro-3-hydroxybutanoate and its derivatives by a robust NADH-dependent reductase from E. coli CCZU-K14,
Bioresource Technology,
Volume 161,2014, Pages 461-464, ISSN 0960-8524,
https://doi.org/10.1016/j.biortech.2014.03.133.
(https://www.sciencedirect.com/science/article/pii/S0960852414004386)

>NZ_CP019420.1:c1644728-1643961 *Mycobacterium* sp. MS1601 chromosome, complete genome

ATGAGCAAGCGTTCCCCGTTCGATCTCTCCGGCCGCACCGCACTGGTGACCGGTGGCAACCAGGGCCTGG
GCCTGGCTTTCGCCTTCGGGCTCGCGGAGGCGGGTGCCACAGTGGCCATCGCCGGCCGCAGTGCTGAACG
CAACGAGAAAGTGGTCGCGGAAGCGGCTGCTCAAGGCCACACCTTCCACGCCATCACTGCCGACATCACC
AAGTCCGAGGACGTGGAATCGATGACCGCCGACGCCATCTCGGCGCTCGGGCACCTCGACATCCTGGTGA
ACAACGCGGGCACCTGCTACCACGGCGAGTCGTGGACGGTGAAGGAGTCCGAGTGGGACGCGGTGTTCGA
TCTCAACGTCAAGGCGCTGTGGGCCTGCTCGCTGGAGGCGGGCAAGCACATGCGTGAGCGCGGCAGCGGC
TCCATCATCAACATCGGCTCGATGTCGGGCATGATCGTCAACCGCCCGCAGATGCAGCCGGCCTACAACG
CCTCCAAGGCCGCGGTGCACCACCTCACCAAATCCCTTGCCGCCGAATGGGGTCCGCTGGGCATCCGGGT
CAACGCACTGGCCCCGGGCTACTGCAAGACCGAGATGGCGCCAGTGGACCGGCCCGAGTTCAAGCAGCAC
TGGATCGACGACACCCCGATGCTGCGCTACGCCATGCCTGAGGAGATCGCCCCGTCGGTGGTGTTCCTGG
CCAGCGACGCCTCGTCCTTCATCACCGGTTCGGTGCTGGTGGCCGACGGGGGTTACACCGCATGGTAG

Protein sequence

Compute pI/Mw
Theoretical pI/Mw (average) for the user-entered sequence:

```
     10         20         30         40         50         60
MSKRSPFDLS GRTALVTGGN QGLGLAFAFG LAEAGATVAI AGRSAERNEK VVAEAAAQGH

     70         80         90        100        110        120
TFHAITADIT KSEDVESMTA DAISALGHLD ILVNNAGTCY HGESWTVKES EWDAVFDLNV

    130        140        150        160        170        180
KALWACSLEA GKHMRERGSG SIINIGSMSG MIVNRPQMQP AYNASKAAVH HLTKSLAAEW

    190        200        210        220        230        240
GPLGIRVNAL APGYCKTEMA PVDRPEFKQH WIDDTPMLRY AMPEEIAPSV VFLASDASSF

    250
ITGSVLVADG GYTAW
```

Theoretical pI/Mw: 5.46 / 27095.65

Table A: Primers for amplification from Mycobacterium genome

Name	Primer Sequence	Tm

GRD_MYC_Forward	gcgcCATATGAGCAAGCGTTCCCCGTTCGATCTCTCC	67 ºC
RGD_MYC_Reverse	gcgcCTCGAGCCATGCGGTGTAACCCCCGTCGGC	69 ºC

Table B: PCR reaction conditions and cycles

Components		**Volume µl**	
DMSO	-	1.5 µL	3 µL
Forward primer	2.5 µL	2.5 µL	2.5 µL
Reverse primer	2.5 µL	2.5 µL	2.5 µL
Template DNA*	1 µL	1 µL	1 µL
PhusionTM Plus DNA Polymerase	0.5 µL	0.5 µL	0.5 µL
Water, nuclease-free	32.5 µL	31 µL	29.5 µL
5X PhusionTM Plus Buffer	10 µL	10 µL	10 µL
10 mM dNTPs	1 µL	1 µL	1 µL
Total	50 µl	50 µl	50 µl

*DNA template is Mycobacterium sp. MS1601 bacterial genome

PCR cycles

Step	**Temperature (˚C)**	**Time**	**Cycles**
Initial denaturation (cell denaturation)	98	3 min	1
Denaturation (DNA denaturation)	98	30 s	
Annealing	72	30 s	34
Extension	72	1 min	
Final extension	72	10 min	1

Table C: Double digestion using fast digest enzymes

Component	**Vector**	**Insert**
H2O	12µl	15µl
10X FastDigest® buffer	2µl	3µl
DNA	3µl	10 µl
XhoI	1µl	1µl

NedI	1µl	1µl
Total volume	20	30

Table D: Ligation Protocol from New England Biolabs (NEB)

Prepare the following reaction mixture in a microcentrifuge tube on ice, adding T4 DNA Ligase last. Use NEBioCalculator to determine the molar ratio, aiming for a 1:3 vector-to-insert ratio for the specified DNA sizes.

Component	**20 µl Reaction**
T4 DNA Ligase Buffer (10X)*	2 µl
Vector DNA (4 kb)	50 ng (0.020 pmol)
Insert DNA (1 kb)	37.5 ng (0.060 pmol)
Nuclease-free water	to 20 µl
T4 DNA Ligase	1 µl

 Thaw and resuspend the T4 DNA Ligase Buffer at room temperature.
 Gently mix the reaction by pipetting up and down, then briefly centrifuge.
 For cohesive (sticky) ends, incubate at 16°C overnight or at room temperature for 10 minutes.
 For blunt ends or single base overhangs, incubate at 16°C overnight or at room temperature for 2 hours. Alternatively, use high concentration T4 DNA Ligase for a 10-minute ligation.
 Heat inactivate the reaction at 65°C for 10 minutes.
 Chill on ice and transform 1-5 µl of the reaction into 50 µl of competent cells.

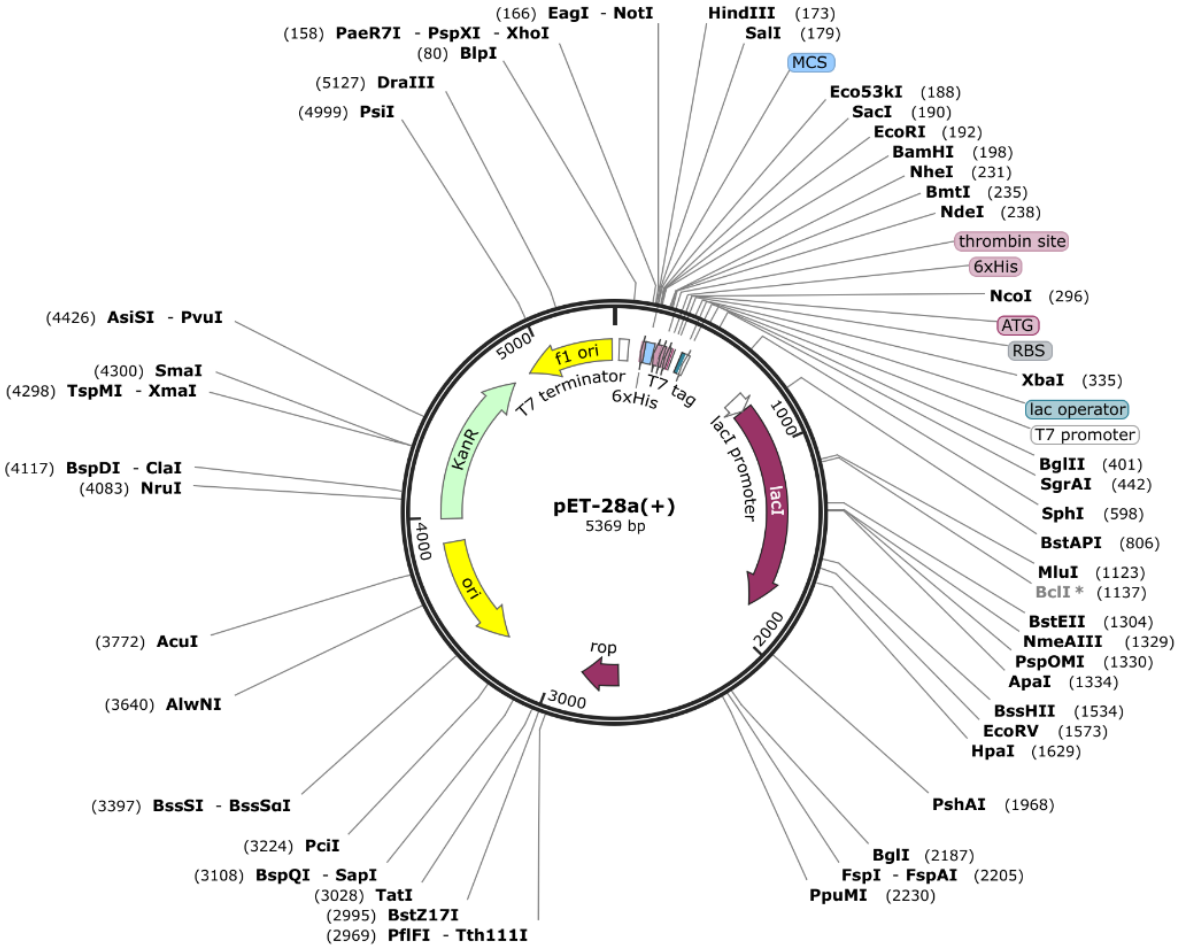

Figure 15: pET-28a+ Vector map from Snap gene

Table D: Chemicals used throughout experiments and theirs sources

Chemical	Source
Sodium hydrogen phosphate (Na2HPO4)	Thermo Scientific™, USA
DMSO	Thermo Scientific™, USA
10mM dNTPs	Thermo Scientific™, USA
DreamTaq Green PCR Master Mix (2X)	Thermo Scientific™, USA
GeneRuler DNA ladder mix	Thermo Scientific™, USA
5X Phusion High Fidelity Buffer	Thermo Scientific™, USA
β-Nicotinamide adenine dinucleotide phosphate sodium salt hydrate (NADP)	Tokyo Chemical Industry, Japan
T7 primers	Eurofins
Yeast extract powder	Warkem biotech, India
Glycerol bidistilled 99.5%	VWR chemicals, USA
Glucose	Sigma-Aldrich
Sorbitol	Sigma-Aldrich
Glycerol	Merck
beta-Nicotinamide adenine dinucleotide, disodium salt, hydrate, 95+%, reduced form	Thermo Scientific™, USA